UILU-ENG-79-2018

CIVIL ENGINEERING STUDIES
STRUCTURAL RESEARCH SERIES NO. 475

A STUDY OF SAFETY OF BOX GIRDER BRIDGES IN JAPAN

By
M. KANAI
and
A. H-S. ANG

Technical Report of Research
Supported by the
NATIONAL SCIENCE FOUNDATION
under
Grant ENV 77-09090

DEPARTMENT OF CIVIL ENGINEERING
UNIVERSITY OF ILLINOIS
at URBANA-CHAMPAIGN
URBANA, ILLINOIS
DECEMBER 1979

A STUDY OF SAFETY OF BOX GIRDER BRIDGES IN JAPAN

By

M. Kanai

and

A. H-S. Ang

Technical Report of Research

Supported by the

NATIONAL SCIENCE FOUNDATION

under

Grant ENV 77-09090

DEPARTMENT OF CIVIL ENGINEERING
UNIVERSITY OF ILLINOIS at URBANA-CHAMPAIGN
Urbana, Illinois

June, 1979

Acknowledgments

This report is based on the dissertation of Michio Kanai submitted to the Graduate College for the M.S. degree. The study was conducted as part of a research program supported by the National Science Foundation under Grant ENV 77-09090.

Much of the data used in the study were provided by the Public Works Research Institute of the Japanese Ministry of Construction; in this regard, the interest and assistance of Dr. Kunihiro, Former Head of the Structure and Bridge Department of the Research Institute, and Mr. Saeki, Head of the Bridge Division of the Institute are gratefully acknowledged.

TABLE OF CONTENTS

LIST OF TABLES

LIST OF FIGURES

CHAPTER 1

INTRODUCTION

1.1 Design Problems of Steel Box Girder Bridges

Because of their structural efficiency, steel box girder bridges have become popular as a bridge type. Since the four unfortunate failures of box girder bridges in the late 1960's and the early 1970's, the behavior of box girder bridges have been widely examined and perhaps is one of the best understood types of bridges today.

Two major problems are particularly significant in the design of box girder bridges, namely the problem of effective width and the adequacy of the linear buckling theory. These have been intensively examined and the results are reflected in many design recommendations and specifications (Lally, 1973; Report of the ASCE-AASHO Task Committee of Flexural Members, 1971; Report of the Task Committee on Orthotropic Plate Bridges, 1974; Report of the Merrison Committee, 1973; AASHTO, 1977).

Although the understanding of the behavior of box girder bridges and associated design methods have recently improved significantly, there remains the important problem of the determination of the proper safety factors for design. Even if the design method is excellent, this problem is important because there are unavoidable uncertainties in the resistance and in the loadings of box girder bridges. For example, non-linear buckling theory gives good estimation of the buckling strength of a stiffened plate, if information about residual stresses and initial deflections is available. Actually, designers have no way to control nor determine the residual stresses or initial deflections in the process of design. The Merrison Report (1973) made it a rule to measure residual stresses and initial deflections of box girder bridges during erection. However, it significantly increases the cost of construction and, therefore, is regarded as impractical.

There is also significant uncertainty in the loadings of box girder bridges. In the design of a bridge girder, the uncertainty in the live load is most significant. Live load which is almost twice the design live load has been reported on national highways in Japan (Ministry of Construction, 1971). In the design of piers, earthquake load is another factor that contributes to the uncertainty in design.

Therefore, it cannot be overemphasized that even if the understanding of the behavior of box girders has significantly improved, uncertainties in design will remain, The appropriate safety factors ought to be derived through an explicit evaluation and systematic analysis of these uncertainties.

1.2 Scope of Report

Although the importance of adequate safety factors in the design of box girder bridges has been recognized, few research studies have been made for this purpose. The Public Works Research Institute of the Ministry of Construction, Japanese Government,has recently performed a number of tests, the results of which may be used in the reliability analysis of box girder bridges. The present study is a reliability analysis of box girder bridge design in Japan using these data.

Two limit states of a stiffened plate are considered, that is the limit state of ultimate strength and the limit state of serviceability. These limit states are affected by many factors, such as initial deflections and residual stresses. The proper resistance factors for the appropriate limit states are discussed based on the available data and in the light of the corresponding uncertainties.

Secondly, the lifetime maximum live load and earthquake load are simulated based on the data and reasonable load factors are presented.

Finally, the safety of box girder bridges designed according to the present specifications (Japan Road Association, 1973) is examined and the underlying consistency is examined and discussed.

Although the importance of the following factors in design is recognized, they are not discussed in detail in this paper.

1. Effective width
2. Impact coefficient
3. Post-buckling strength
4. Erection
5. Structural details

CHAPTER 2

RESISTANCE OF BOX GIRDER BRIDGES

2.1 Description of Experimental Program

Large-scale experiments of stiffened plates were performed by the Public Works Research Institute, Ministry of Construction of the Japanese Government during 1975 and 1977. The objective of the experiment was to determine the strength characteristics of a stiffened plate to resist strong-motion earthquakes. In order to reflect actual fablication and erection condition, 45 large specimens were tested, using 1000-ton capacity testing machine. A summary of the test results has been published (P.W.R.I., 1977).

A typical configuration of the test specimens is shown in Fig. 2.1. All the specimens are stiffened box girders. At both ends, the specimens are elaborately stiffened in order to insure that no buckling occurs at the end panels. Uniformly distributed compression is applied at both edges of the specimens. However, in spite of great care in finishing the ends of the specimens, the applied stresses may not be perfectly uniform. In the tests, the experimental condition was judged to be satisfactory, if the stress variation at various points of a specimen is less than 10%.

The complete list of dimensions of the specimens is shown in Table 2.1. The 45 specimens in the test program were intended to cover all the ranges of the design variables. They were fablicated by three different fablicators to reflect different fabrication conditions. The material used was SS41, a mild structural steel with 41kg/cm^2 ultimate strength. The number of stiffeners varies from 0 to 3, and the breadth-to-thickness ratio of the panels varies from 30 to 230. The ratio γ/γ^* of the stiffeners (γ is the ratio of the stiffener stiffness to the panel stiffness, while γ^* is the DIN specified stiffener stiffness) varies from 0.1 to 10.0. The aspect ratio of the panels varies from 2.0 to 5.5.

Some of the specimens have hybrid stiffeners whereas others have T-shape stiffeners. Higher stiffener stiffness are expected with the hybrid stiffeners whereas T-shape stiffeners were used for greater warping resistance.

During the experiment, the strain of the panels, out-of-plane deflection of the panels, total length of the specimens and lateral displacement of the stiffeners were measured and recorded.

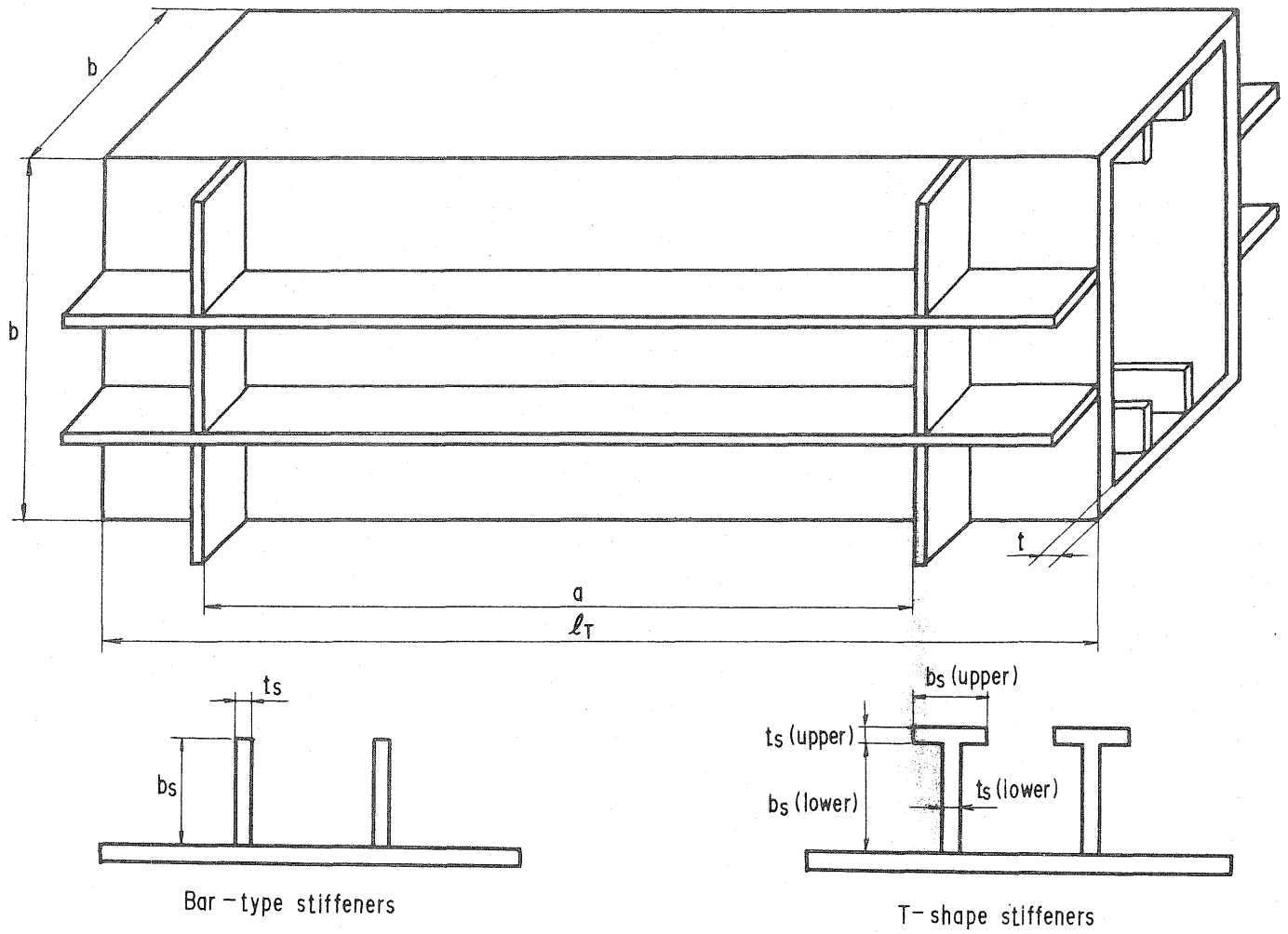

Fig. 2.1 TYPICAL CONFIGURATION OF TEST SPECIMENS

2.2 Description and Discussion of Test Results

As discussed in many papers, the limit states of a stiffened plate cannot be explained by elastic buckling theory, because stiffened plates used in box girder bridges are very thin and affected by many imperfections including residual stresses and initial deflections. Elasto-plastic buckling theory, therefore, will be needed to explain properly the resistance characteristics of a stiffened plate.

However, in elasto-plastic buckling theory, simple expression of the limit states is almost impossible. Furthermore, information on the magnitude of residual stresses and initial deflections is needed to apply the theory. So, although the elasto-plastic theory is more exact for determining the limit states, it may not be practical for design purposes.

In specifications, therefore, the specified limit states are usually based on the elastic theory, modifying the elastic design curves by the results of elasto-plastic analysis. In this report, the same procedure is adopted. First, elastic design variables are introduced. These are subsequently modified with the results of experiments.

The design variables used in this report are as follows.

1. N = number of stiffeners in a panel
2. R_R = equivalent breadth-to-thickness ratio for the R-mode buckling (R-mode buckling, as shown in Fig. 2.2, is buckling of subpanels between straight stiffeners) given by

$$R_R = \frac{b}{t}\sqrt{\frac{\sigma y}{E} \cdot \frac{12(1-\nu^2)}{\pi^2 k_R}} \tag{2.1}$$

where:

b = breadth of a panel

t = thickness of a panel

σy= yield point of material

E = modulus of elasticity

ν = Poisson's ratio

k_R= buckling coefficient for R-mode; $k_R = 4n^2$

n = number of sub-panels between stiffeners

In the elastic buckling theory, the R-mode buckling strength of a stiffened plate is expressed as follows.

$$\sigma cr/\sigma y = 1/R_R^2 \tag{2.2}$$

Observe that for $R_R = 1.0$, the R-mode elastic buckling strength is equal to the yield point of the material.

3. R_F = equivalent breadth-to-thickness ratio for F-mode buckling

(F-mode buckling, also shown in Fig. 2.2, is the general buckling of the entire stiffened panel) given by

$$R_F = \frac{b}{t}\sqrt{\frac{\sigma y}{E} \cdot \frac{12(1-\nu^2)}{\pi^2 k_F}} \tag{2.3}$$

where:

$$k_F = \begin{cases} \dfrac{(1+\alpha^2)^2+\eta\gamma}{\alpha^2(1+\eta\delta)} & ; \quad \alpha < \sqrt[4]{1+\eta\gamma} \\ \dfrac{2(1+\sqrt{1+\eta\gamma})}{1+\eta\delta} & ; \quad \alpha \geqq \sqrt[4]{1+\eta\gamma} \end{cases}$$

in which

γ = ratio of stiffener stiffness to panel stiffness

α = aspect ratio of a panel ; $\alpha = a/b$

δ = ratio of the area of a stiffener to the area of a panel

The F-mode buckling strength is expressed by the following formula.

$$\sigma cr/\sigma y = 1/R_F^2 \tag{2.4}$$

4. R_{max} = the maximum of R_R and R_F, which determines the elastic buckling strength of a stiffened plate.

$$R_{max} = \max (R_R, R_F) \tag{2.5}$$

The elastic buckling strength of a stiffened plate is, therefore, expressed by the following.

$$\sigma cr/\sigma y = 1/R_{max}^2 \tag{2.6}$$

5. γ/γ^* = the ratio of a stiffener stiffness (γ) to the DIN specified stiffener stiffness (γ^*).

The DIN specified stiffener stiffness is determined so that the R-mode buckling strength is equal to the F-mode buckling strength. Therefore, γ^* gives the optimum stiffener stiffness as far as elastic design is concerned.

Values of the design variables for 45 specimens are shown in Table 2.2.

Fig. 2.3 shows a typical plot of the experimental data, from which the following limit states can be observed.

1. The ultimate or the maximum strength of a specimen (U).

2. The stress at which local plastic flow begins (P). This kind of local plastic flow can be seen in many structural members even at low stress level.
3. Bifurcation (B), which is the separation of strain curves as shown in Fig. 2.3. The initiation of bifurcation usually coincides with the out-of-plane deflection of panels or loss of rigidity. Sometimes, buckling is defined by the bifurcation point.
4. The beginning of out-of-plane deflection (D). Usually, this is the same as the bifurcation point.
5. The loss of rigidity (R), which means the loss of rigidity as a column.

Values of these limit states are shown in Table 2.2. Due to errors of measurement, B, D and R do not necessarily coincide with each other; however, such errors are usually small.

Fig. 2.4 shows the plot of the ultimate strength in terms of $\sigma cr/\sigma y$ against Rmax. If the buckling of a stiffened plate is elastic, the plot should coincide with the Euler buckling curve, which is also shown in Fig. 2.4. Because of the effects of imperfections and non-linearity, the results deviate from the Euler curve at lower Rmax. Further, it may be ovserved that there is considerable scatter in the ultimate strength.

Besides the information given in Table 2.2 the following information can be derived also from the results of the experiments.

First, as shown typically in Fig. 2.5, out-of-plane deflections can be observed even at low stresses for specimens with high R_R values (R_R=1.36). The reason for this instability is that the effects of imperfections are extremely significant in very thin plates. For this very reason, stiffened plates with high R_R values are not suitable for structural purposes, and therefore, should be avoided in design.

Secondly, as demonstrated in Fig. 6, the post-buckling strength of the specimens with low R_R value are quite stable (see curve A with R_R=0.52), even when subjected to repeated loads. However, the post-buckling strength of the specimens with high R_R value (curve B with R_R=1.36) are not reliable when subjected to repeated loads.

From these results, the use of a stiffened plate with high R_R value is not recommended. These conclusion will be reflected in the design curves developed in the subsequent chapters.

Table 2.1 DIMENSIONS AND PARAMETERS OF TEST SPECIMENS

#	N	σy	t	b	a	ℓ_T	σys	ts	bs	γ^*	γ/γ^*	k_R	k_F	Py
1	0	2860	6	169	400	600	-	-	-	-	-	4.0	-	112
2	0	2860	6	236	500	700	-	-	-	-	-	4.0	-	158
3	1	2860	6	337	700	900	2860	6	27	27.0	0.22	16.0	7.9	246
4	1	2860	6	472	1400	1800	2860	6	55	39.9	0.90	16.0	15.4	358
5	2	2860	6	304	600	800	2860	6	19	48.3	0.05	36.0	6.4	231
6	2	2860	6	506	1700	2100	2860	6	58	132.5	0.30	36.0	17.7	423
7	2	2980	6	709	3900	4300	2990	10	107	312.3	0.94	36.0	34.9	759
8	2	3100	6	1012	3900	4300	2990	10	113	194.8	1.24	36.0	42.2	1019
9	2	3100	6	506	1700	2100	3100	6	67	139.7	0.43	36.0	21.1	472
10	2	3100	6	506	1700	2100	3260	8	87	179.2	0.99	36.0	35.8	554
11	2	3100	6	709	3900	4300	3990	10	107	312.3	0.94	36.0	35.0	865
12	2	3100	6	709	3900	4300	2930	11	130	404.6	1.43	36.0	44.6	858
13	2	3100	6	709	3900	4300	2610	13	155	554.5	2.09	36.0	60.8	944
14	3	2790	6	404	1100	1400	2790	6	35	142.6	0.08	64.0	11.4	337
15	3	2790	6	674	3600	4000	3260	8	97	589.5	0.31	64.0	31.8	751
16	2	2800	8	529	1058	1586	3870	6	48	50.2	0.18	36.0	10.8	566
17	2	2800	8	529	1058	1586	2800	8	84	63.4	1.01	36.0	36.8	617
18	2	2800	8	529	1058	1586	2800	8	104	68.8	1.77	36.0	61.4	653
19	2	2800	8	661	1322	1982	3870	6	66	51.2	0.37	36.0	16.6	708
20	2	2800	8	661	1322	1982	2800	8	88	59.6	0.99	36.0	36.1	743
21	2	2800	8	661	1322	1982	3080	9	108	67.0	1.83	36.0	63.4	825
22	2	3870	6	595	1190	1784	3870	6	59	54.7	0.64	36.0	25.1	657
23	2	3870	6	595	1190	1784	3870	6	69	57.2	0.98	36.0	35.9	675
24	2	3870	6	595	1190	1784	2800	8	80	66.3	1.76	36.0	61.1	690
25	2	3880	6	694	1388	2082	3880	6	72	55.4	0.99	36.0	36.1	775
26	2	3880	6	694	1388	2082	2800	8	84	63.7	1.82	36.0	62.8	791
27	2	3880	6	1389	2778	4166	3880	6	84	49.1	0.89	36.0	32.9	1444
28	2	2800	8	529	1058	1586	4130	8	84	63.4	1.01	36.0	36.8	689
29	2	2800	8	661	1322	1982	4130	8	88	59.6	0.99	36.0	36.1	818
30	2	3880	6	592	1190	1784	4130	8	64	61.2	0.98	36.0	35.7	718
31	2	3880	6	694	1388	2082	4130	8	68	59.3	1.04	36.0	37.6	820
32	2	3150	8	500	999	1399	3060	8	82	64.5	0.96	36.0	35.1	675
33	2	3150	8	500	999	1399	2863	10	105	79.4	2.06	36.0	71.5	760
34	2	3150	8	624	1250	1650	3060	8	87	61.1	0.97	36.0	35.4	813

#	N	σy	t	b	a	ℓ_T	σys	ts	bs	γ^*	γ/γ^*	k_R	k_F	Py
35	2	3125	8	625	1246	1646	2863	10	110	72.7	2.07	36.0	71.5	896
36	2	2930	8	750	1500	1900	2933	9	83	59.6	0.92	36.0	33.8	914
37	2	2930	8	749	1499	1899	2863	10	116	68.4	2.05	36.0	70.4	1000
38	2	3100	8	750	1499	1899	3217	6 / 6	62* / 67	58.7	0.92	36.0	33.7	987
39	2	3083	6	634	1267	1667	3217	6	72	56.6	0.93	36.0	34.3	609
40	2	3085	6	633	1268	1668	3153	6 / 6	43* / 48	61.8	0.92	36.0	33.9	642
41	2	3140	6	724	1448	1848	3153	6 / 6	46* / 51	59.9	0.94	36.0	34.4	742
42	2	3082	6	1045	2170	2570	3080	8	72	58.6	0.94	36.0	34.7	901
43	2	3177	6	1117	2354	2754	3100	8	73	59.3	0.91	36.0	33.5	983
44	2	3147	6	1267	2501	2901	3060	8	79	51.1	0.93	36.0	34.1	1163
45	2	3147	6	1267	2536	2936	3217	6 / 6	52* / 57	52.9	0.91	36.0	33.8	1178

---

* For T-shape stiffeners, upper number is the dimensions of flanges; whereas lower number refers to the dimensions of webs.

: specimen number
N : number of stiffeners
σy : yield point of panels (kg/cm^2)
t : thickness of panels (mm)
b : breadth of panels (mm)
a : length of panels (mm)
ℓ_T : total length of a specimen (mm)
σys: yield point of stiffeners (kg/cm^2)
ts : thickness of stiffeners (mm)
bs : breadth of stiffeners (mm)
γ^* : DIN specified stiffener stiffness (relative to panel stiffness)
γ : stiffener stiffness (relative to panel stiffness)
k_R : buckling coefficient for R-mode (rigid mode)
k_F : buckling coefficient for F-mode (flexible mode)
Py : net section yield load (ton)

Test specimen #28, 29, 30 and 31 have hybrid stiffeners, whereas specimen #38, 40, 41, 45 have T-shape stiffeners.

Table 2.2 DESIGN VARIABLES AND LIMIT STATES

#	N	R_R	R_F	γ/γ^*	U	P	B	D	R	Stiffener
1	0.	.55	-1.00*	-1.00*	1.13	.62	1.04	1.08	1.08	-**
2	0.	.76	-1.00*	-1.00*	.91	.76	.88	.88	.80	-
3	1.	.55	.78	.22	.98	.32	.78	.86	.80	-
4	1.	.76	.78	.90	.90	.54	.62	.74	.68	-
5	2.	.33	.78	.04	1.06	.54	.72	.78	.72	-
6	2.	.55	.78	.29	.87	.56	.62	.56	.56	-
7	2.	.78	.79	.94	.89	-1.00*	.54	.54	.54	-
8	2.	1.14	1.05	1.24	.65	.56	.62	.54	.62	-
9	2.	.57	.74	.44	.87	.48	.66	.60	.70	-
10	2.	.57	.57	.98	.87	.44	.68	.66	.72	-
11	2.	.80	.81	.94	.84	.30	.46	.48	.58	-
12	2.	.80	.72	1.43	.84	.40	.40	.42	.56	-
13	2.	.80	.61	2.09	.87	.58	.62	.58	.62	-
14	3.	.32	.77	.08	1.03	.82	.90	.90	.90	-
15	3.	.54	.76	.31	.86	-1.00*	.56	.48	.60	-
16	2.	.42	.77	.18	1.01	.58	.78	.78	.80	-
17	2.	.42	.42	1.02	1.29	.72	.80	.86	.82	-
18	2.	.42	.32	1.77	1.23	.60	.90	.90	.90	-
19	2.	.53	.78	.37	.88	.56	.70	.65	.72	-
20	2.	.53	.53	.98	1.07	.50	.60	.56	.86	-
21	2.	.53	.40	1.84	1.03	.72	.80	.85	.90	-
22	2.	.75	.80	.64	.69	.54	.64	.48	.64	-
23	2.	.75	.75	.98	.72	.36	.66	.46	.62	-

#	N	R_R	R_F	γ/γ^*	U	P	B	D	R	Stiffener
24	2.	.75	.57	1.77	.85	.30	.60	.56	.60	-
25	2.	.87	.87	1.00	.66	.28	.48	.40	.40	-
26	2.	.87	.66	1.81	.82	.38	.52	.52	.52	-
27	2.	1.74	1.83	.88	.36	.10	.20	.14	.30	-
28	2.	.42	.42	1.02	1.22	.56	.70	.70	.76	Hybrid
29	2.	.53	.53	.98	1.01	.46	.60	.56	.72	Hybrid
30	2.	.75	.75	.98	.80	.44	.62	.58	.56	Hybrid
31	2.	.87	.85	1.05	.77	.26	.42	.42	.60	Hybrid
32	2.	.42	.42	.96	.95	.72	.80	.80	.82	-
33	2.	.42	.30	2.06	.99	.52	.80	.80	.76	-
34	2.	.52	.52	.97	.92	.62	.62	.68	.68	-
35	2.	.52	.37	2.07	.96	.72	.72	.68	.72	-
36	2.	.59	.61	.92	.95	.50	.60	.68	.64	-
37	2.	.59	.42	2.06	.99	.58	.72	.72	.76	-
38	2.	.60	.64	.92	.94	.64	.68	.70	.68	T-shape
39	2.	.67	.69	.93	.86	.62	.62	.60	.62	-
40	2.	.67	.69	.92	.90	-1.00	.60	.62	.60	T-shape
41	2.	.76	.77	.93	.86	.54	.62	.48	.62	T-shape
42	2.	1.20	1.22	.93	.58	.36	.36	.30	.36	-
43	2.	1.30	1.35	.92	.54	.28	.36	.24	.28	-
44	2.	1.36	1.40	.92	.55	.18	.36	.32	.36	-
45	2.	1.36	1.41	1.04	.56	.36	.36	.40	.44	T-shape

* - 1.0 means no data

** - means bar-type stiffener

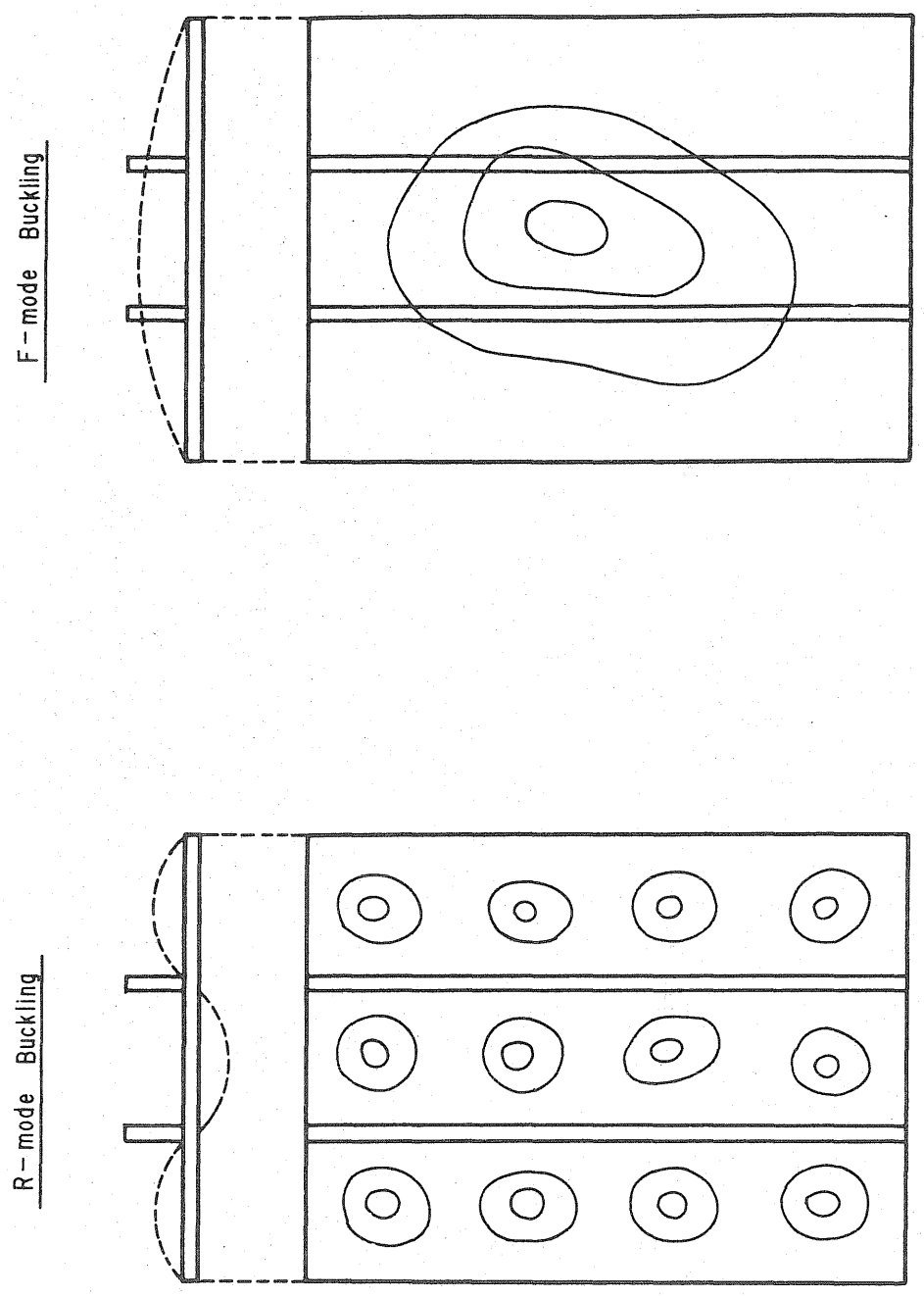

Fig. 2.2 BUCKLING MODES

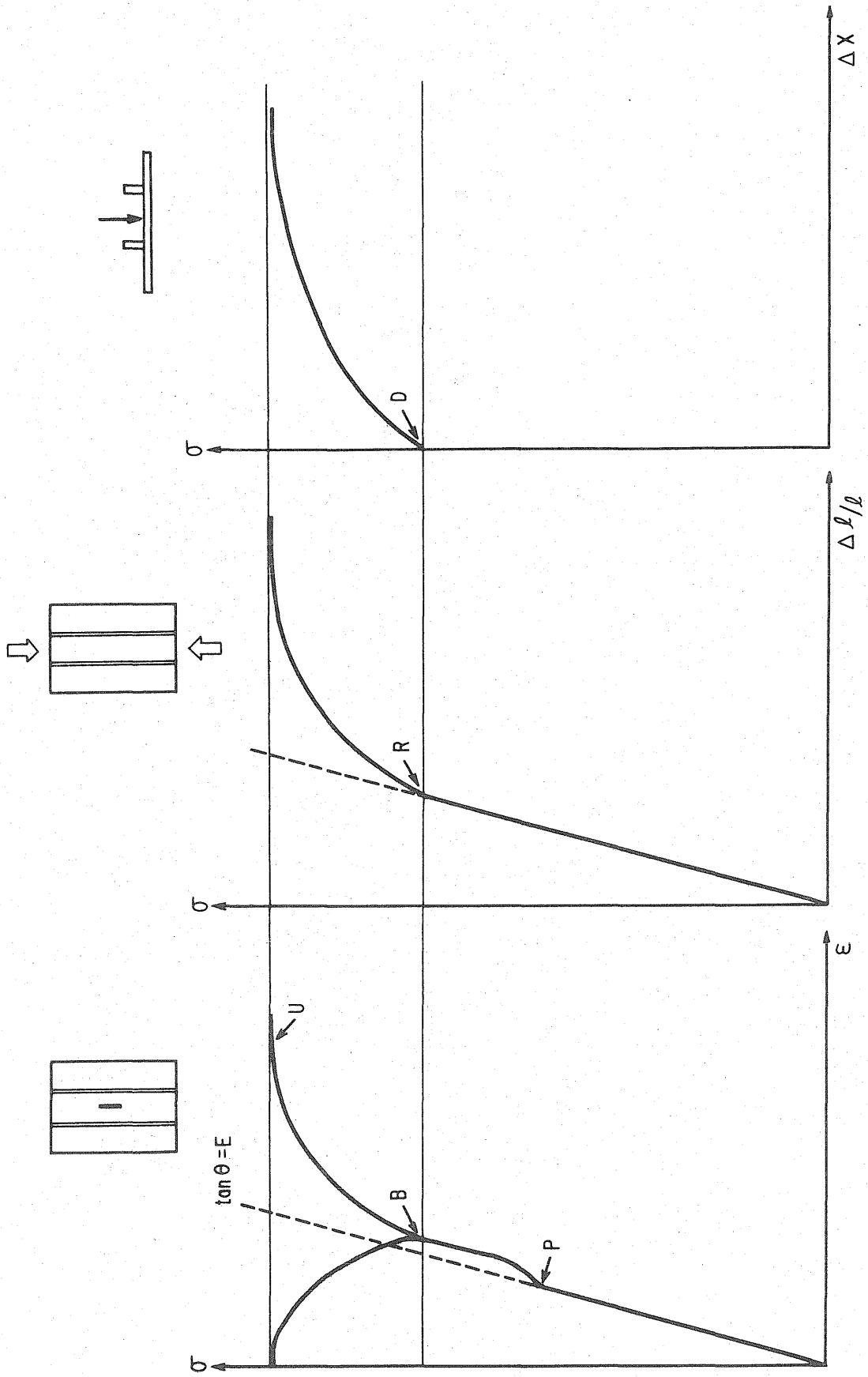

Fig. 2.3 LIMIT STATES

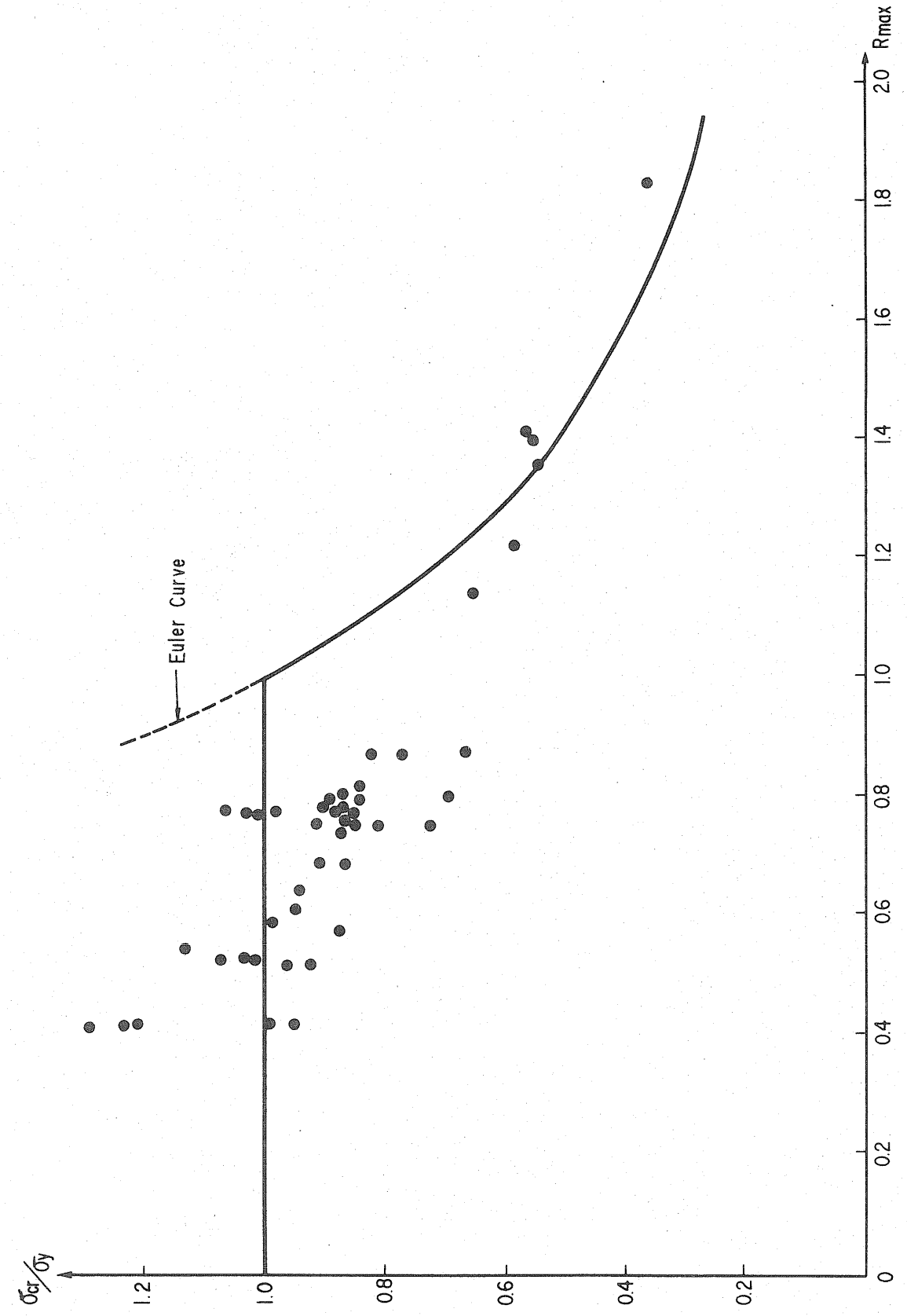

Fig. 2.4 ULTIMATE STRENGTH

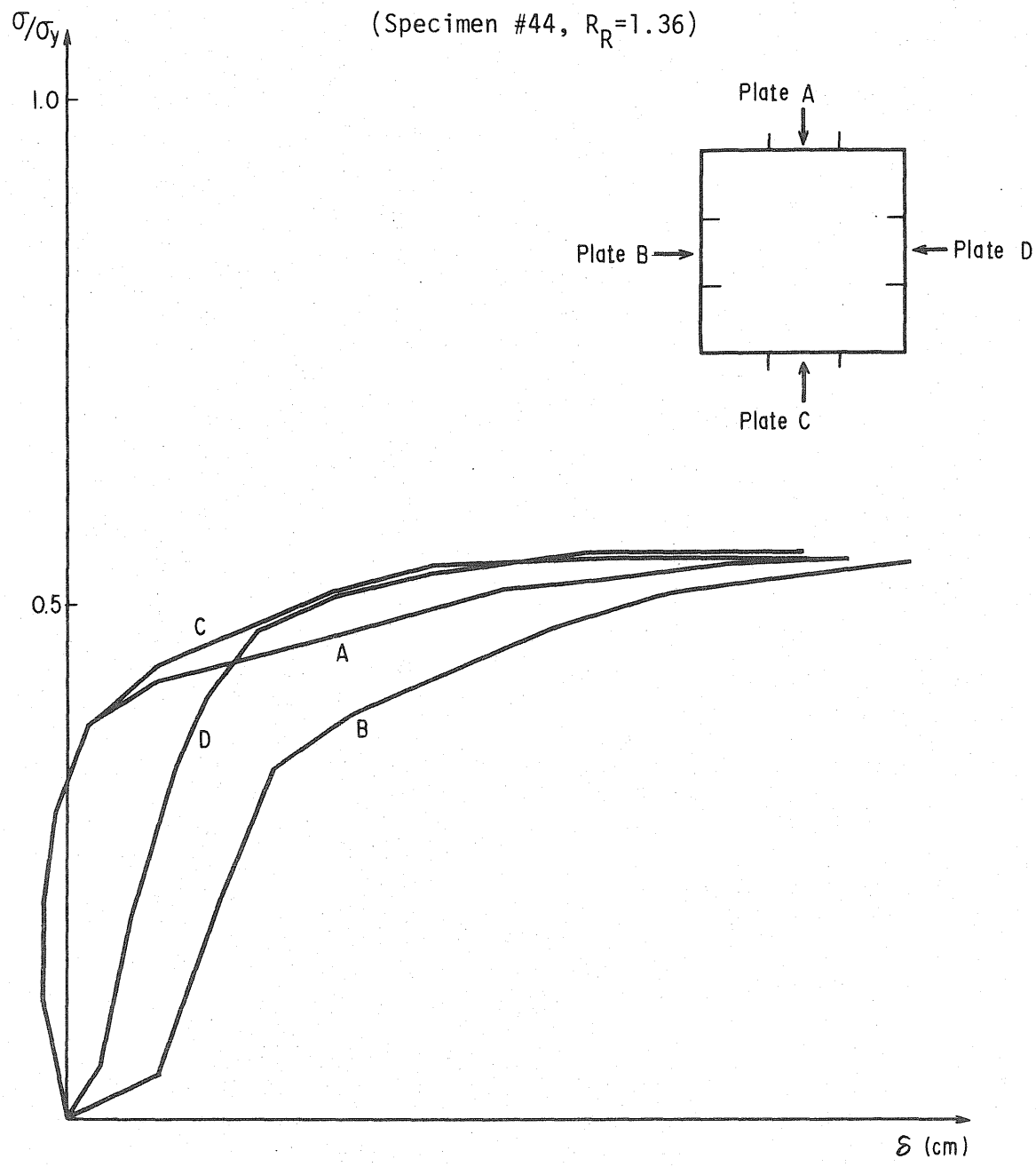

Fig. 2.5 OUT-OF-PLANE DEFLECTION

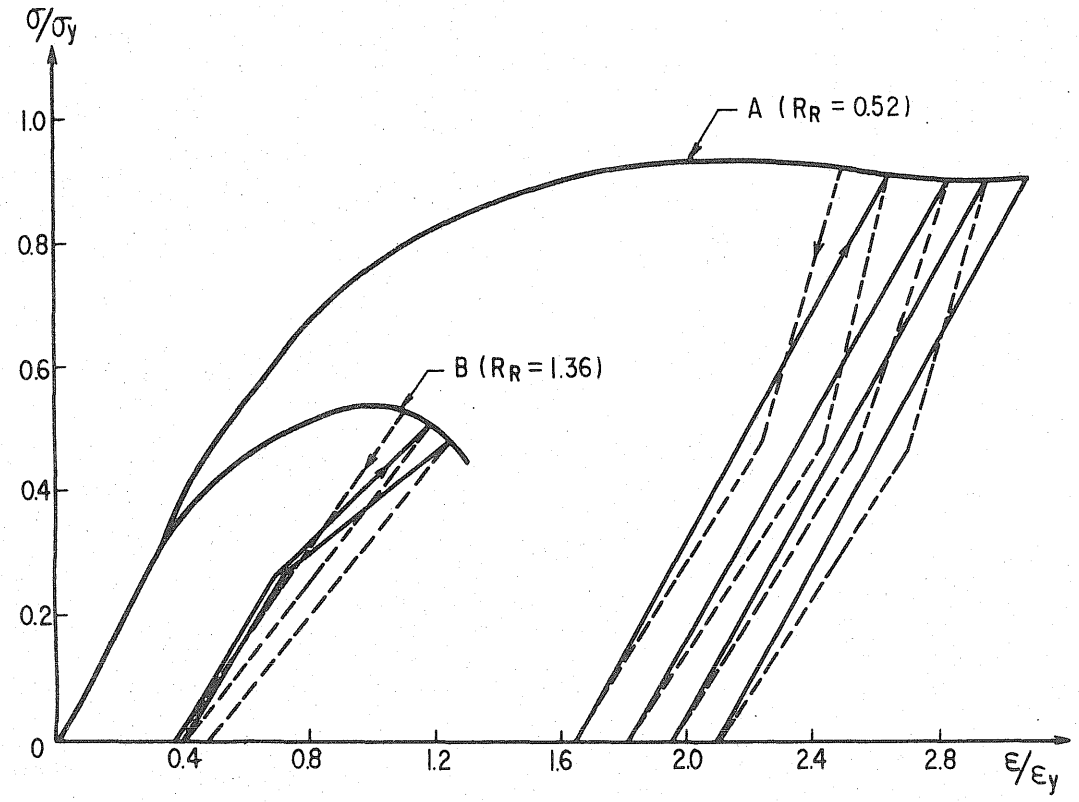

A ; Specimen #34 $R_R = 0.52$

B ; Specimen #44 $R_R = 1.36$

Fig. 2.6 RESISTANCE TO REPEATED LOAD

2.3 Analysis of Test Results

The test data summarized earlier can be used to establish the relationships between the limit states of a stiffened plate and the pertinent design variables. Such relationships are developed herein through nonlinear regression analysis.

2.3.1 Ultimate Strength -- As discussed in the previous chapter, the elastic buckling strength of a stiffened plate may be expressed as follows.

$$\sigma cr/\sigma y = \begin{cases} 1.0 & ; \quad Rmax \leq 1.0 \\ 1/R^2_{max} & ; \quad Rmax > 1.0 \end{cases} \tag{2.7}$$

However, in elasto-plastic buckling, Rmax may not necessarily be the most suitable design variable to express the ultimate strength. Alternative relationships were developed by regression analysis, the results of which may be summarized as follows. All the limit states are expressed as a fraction of the yield point of the material.

In terms of R_R, the ultimate strength regression is;

$$U = -0.119R_R+0.490R^2_R-0.117R^3_R+1.446 \tag{2.8}$$

The conditional standard deviation of U given R_R is $\sigma(U|R_R)=0.081$, and the correlation coefficient is 0.75.

In terms of R_F, the corresponding ultimate strength regression is;

$$U = -0.459R_F-0.139R^2_F+0.067R^3_F+1.259 \tag{2.9}$$

The conditional standard deviation of U given R_F is $\sigma(U|R_F)=0.096$, and the corresponding correlation coefficient is 0.69.

Finally, in terms of Rmax, the ultimate strength regression is;

$$U = -1.121Rmax+0.426Rmax^2-0.086Rmax^3+1.510 \tag{2.10}$$

The conditional standard deviation of U given Rmax is $\sigma(U|Rmax)=0.087$, and the correlation coefficient is 0.73.

From these results, it may be concluded that R_R is the "best" design variable to explain the ultimate strength characteristics, in the sense that this gives the least conditional standard deviation. However, as R_R does not include information on the effects of stiffener stiffness, the following regression equations were obtained to include these effects.

$$\text{For } \gamma/\gamma^*<1.0 \; ; \; U = -0.920R_R+0.277R^2_R-0.046R^3_R+0.071\gamma/\gamma^*+1.307 \tag{2.11}$$

The conditional standard deviation of U given R_R and γ/γ^* is 0.058, and the correlation coefficient is 0.81.

For $\gamma/\gamma^* \geq 1.0$; $U = -1.938R_R+1.036R_R^2-0.226R_R^3-0.053\ \gamma/\gamma^*+1.901$ (2.12)

The conditional standard deviation of U given R_R and γ/γ^* is 0.071, and the correlation coefficient is 0.82.

From these latter results, it is clear that larger stiffener stiffness has positive effects on the ultimate strength up to $\gamma=\gamma^*$. However it has no effect beyond that point. So, the DIN specified γ^* is a very reasonable stiffness parameter even for elasto-plastic buckling.

A similar analysis yielded the following regression equations for girders with T-shape stiffeners and hybrid stiffeners.

With T-stiffeners;

$U = -1.500R_R+0.819R_R^2-0.202R_R^3+0.070\gamma/\gamma^*+0.037T+1.496$ (2.13)

with conditional standard deviation of 0.072, and the correlation coefficient of 0.78. The value of the variable T is 1 for the specimens with T-shape stiffeners, and 0 for the specimens with rectangular bar stiffeners.

With hybrid stiffeners;

$U = -1.506R_R+0.839R_R^2-0.210R_R^3+0.069\gamma/\gamma^*+0.051Hy+1.493$ (2.14)

with conditional standard deviation of 0.071, and correlation coefficient of 0.79. The value of the variable Hy is 1 for specimens with hybrid stiffeners and 0 for the specimens with homogeneous stiffeners.

Equations (2.13) and (2.14) indicate that T-shape and hybrid stiffeners have some positive effects on the ultimate strength; however, these effects are small.

From the results of the above analyses, the following may be inferred about the ultimate strength of a stiffened plate:

1. The ultimate strength of a stiffened plate can be explained adequately as a function of R_R and γ/γ^*.
2. Stiffener stiffness has positive effects for $\gamma \leq \gamma^*$; however, these effects are small for $\gamma > \gamma^*$. For these reasons, γ^* is a reasonable upper limit of useful stiffener stiffness.
3. The ultimate strength of a stiffened plate can be estimated by the following formula for $\gamma=\gamma^*$;

   $U = -0.920R_R+0.277R_R^2-0.046R_R^3+1.378$ (2.15)

   The conditional standard deviation of the formula is 0.058.

4. T-shape and hybrid stiffeners have positive effects on the ultimate strength; however, these effects are small.

2.3.2 Serviceability Limits -- Bifurcation, out-of-plane deflection and loss of rigidity may be considered as limit states of serviceability. As these limit states are fundamentally the buckling of sub-panels, or R-mode buckling, it is reasonable to assume that these limit states are functions of R_R. Nonlinear regressions, using the test data summarized earlier, yield the following for the respective serviceability limits.

1. Bifurcation;

$$B = -1.437R_R+0.988R_R^2-0.287R_R^3+1.218 \qquad (2.16)$$

The conditional standard deviation is 0.072. The correlation coefficient is 0.73.

2. Out-of-plane deflection;

$$D = -1.834R_R+1.278R_R^2-0.357R_R^3+1.349 \qquad (2.17)$$

The conditional standard deviation is 0.088. The correlation coefficient is 0.71.

3. Loss of rigidity;

$$R = -0.750R_R+0.141R_R^2-0.019R_R^3+1.082 \qquad (2.18)$$

The conditional standard deviation is 0.074. The correlation coefficient is 0.72.

Stiffener stiffness has no direct effect on the R-mode buckling. However, the rigidity and warping resistance of stiffeners have some effects on the above serviceability limit states. Nonlinear regressions of the test data including these effects result in the following:

1. Bifurcation;

$$B = -1.652R_R+1.179R_R^2-0.338R_R^3+0.042\gamma/\gamma^*+1.244 \qquad (2.19)$$

The conditional standard deviation is 0.069. The correlation coefficient is 0.74.

2. Out-of-plane deflection;

$$D = -2.121R_R+1.534R_R^2-0.426R_R^3+0.056\gamma/\gamma^*+1.384 \qquad (2.20)$$

The conditional standard deviation is 0.083. The correlati n coefficient is 0.73.

3. Loss of rigidity;

$$R = -0.988R_R+0.353R_R^2-0.038R_R^3+0.046\gamma/\gamma^*+1.111 \qquad (2.21)$$

The conditional standard deviation is 0.070. The correlation coefficient is 0.74.

Equation (2.15) is plotted in Fig. 2.7 (a), and equations (2.19) through (2.21) are plotted in Fig. 2.7 (b), assuming $\gamma=\gamma^*$.

T-shape stiffeners and hybrid stiffeners, as may be observed in the following, have negligible effects on the serviceability limit states. This is reasonable and to be expected, because such limit states are determined by R-mode buckling.

With T-shape stiffeners;

$$B = -1.670R_R+1.189R_R^2-0.339R_R^3+0.043\gamma/\gamma^*+0.024T+1.248 \qquad (2.22)$$

The conditional standard deviation is 0.069. The correlation coefficient is 0.74.

With hybrid stiffeners;

$$B = -1.610R_R+1.137R_R^2-0.327R_R^3+0.041\gamma/\gamma^*-0.059Hy+1.239 \qquad (2.23)$$

The conditional standard deviation is 0.067. The correlation coefficient is 0.75.

From the results of the above analyses, the following conclusions may be derived regarding the limit states of serviceability.

1. The limit states of serviceability can be explained adequately as functions of R_R and γ/γ^*.
2. T-shape stiffeners and hybrid stiffeners have no effect on the pertinent serviceability limits.
3. Although there are slight difference between the three serviceability limit states, they can be expressed by the following single equation for $\gamma=\gamma^*$.

   $$\text{Serviceability} = -1.587R_R+1.022R_R^2-0.267R_R^3+1.294 \qquad (2.24)$$

   The total standard deviation** is 0.078.

** This includes the error of Equation (17) in addition to the standard deviation of the original regression equations.

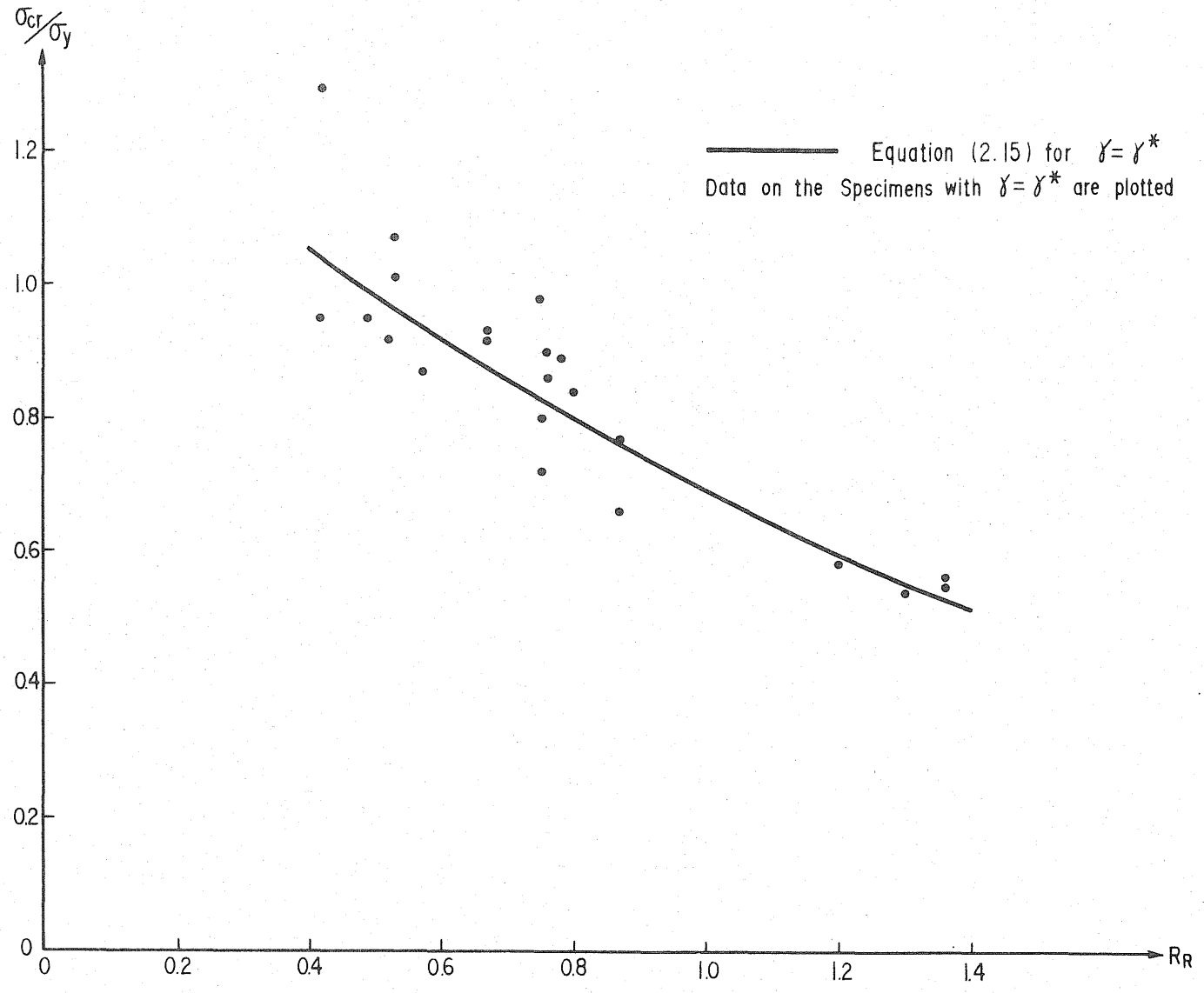

Fig. 2.7(a) ULTIMATE STRENGTH ($\gamma=\gamma^*$)

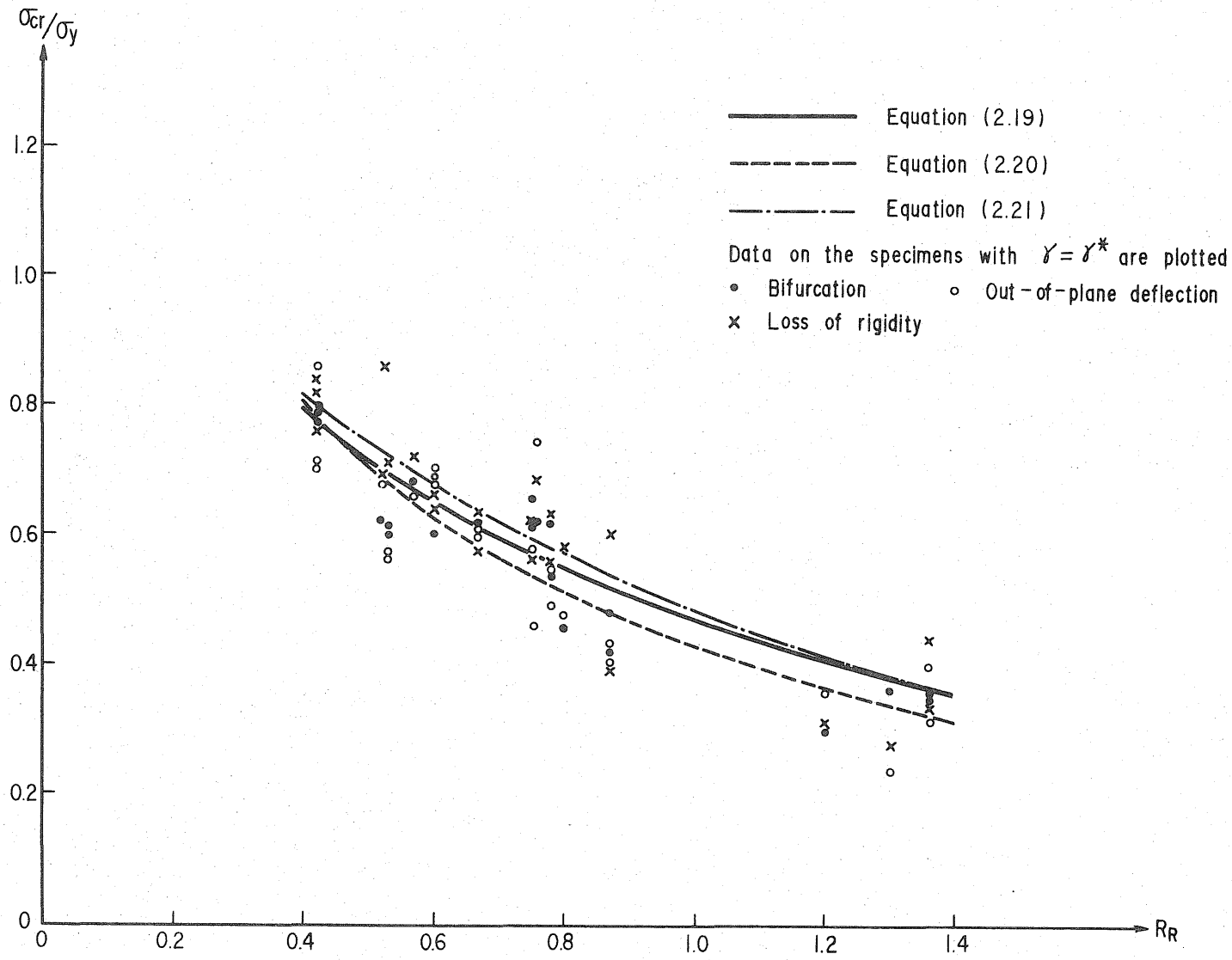

Fig. 2.7(b) SERVICEABILITY LIMITS ($\gamma=\gamma^*$)

CHAPTER 3

LOAD ANALYSIS ON BOX GIRDER BRIDGES

3.1 Live Load on Short-Span Bridges

Wheel load determines the design of slabs, deck plates, stringers and short short-span bridge girders. In Japan, as in many other countries, wheel loads as high as two times the nominal design wheel load (8 tons in Japan) have repeatedly been reported on national highways. A careful analysis of wheel load data for the determination of the lifetime maximum wheel load, therefore, is needed.

The following analysis is limited to the estimation of the lifetime maximum wheel load. The effects of the position of wheel load, which would be important in the design of slabs, is not discussed here; such problems will depend on the type of members, geometry, and many other factors.

The Ministry of Construction of the Japanese Government is continuously collecting data on wheel loads on major national highways in Japan. The latest data (obtained in 1975 and 1977) are now available; about 3 million observations were recorded (P.W.R.I. 1978). The analysis in this chapter is based on this set of data. So, the results of the analysis can be applied to major national highways in Japan. The data are summarized in Table 3.1.

Since the main concern is on the lifetime maximum wheel load, the population of interest may be limited to that of heavy trucks. To obtain the distribution function of heavy trucks, it is reasonable to neglect the data below

Table 3.1 SUMMARY OF WHEEL LOAD DATA

Weight(tons)	Total Number of Observations	Cumulative Probability
0 - 1	1959513	0.7221
1 - 2	2260927	0.8332
2 - 3	2466885	0.9091
3 - 4	2579251	0.9505
4 - 5	2640448	0.9731
5 - 6	2676613	0.9864
6 - 7	2696425	0.9937
7 - 8	2706006	0.9972
8 - 9	2710482	0.9989
9 - 10	2712356	0.9996

Weight(tons)	Total Number of Observations	Cumulative Probability
10 - 12	2713258	0.9999
12 - 14	2713521	1.0000
14 - 16	2713522	1.0000

certain weight. In this regard, three types of distribution functions were examined; in each case, the wheel load data above 4, 6 and 8 tons were used to estimate the parameters of the respective distributions. The three distribution functions considered herein are as follows.

1. Shifted exponential distribution;

$$fx(x) = \lambda \cdot e^{-\lambda(x-Xa)} \quad ; \quad \text{for } x \geq Xa \tag{3.1}$$

where:

Xa = minimum wheel load

2. Tail of the normal distribution;

$$x(x) = \frac{1}{a} \cdot \frac{1}{\sqrt{2\pi}\sigma} \cdot \exp\left[-\frac{1}{2}\left(\frac{x-\mu}{\sigma}\right)^2\right] \; ; \text{ for } x \geq Xa \tag{3.2}$$

where:

Xa = minimum wheel load

$$a = 1 - \Phi\left(\frac{Xa-\mu}{\sigma}\right)$$

3. Tail of the log normal distribution;

$$hx(x) = \frac{1}{a} \cdot \frac{1}{\sqrt{2\pi}\xi x} \cdot \exp\left[-\frac{1}{2}\left(\frac{\ell n x-\lambda}{\xi}\right)\right] \; ; \text{ for } x \geq Xa \tag{3.3}$$

where:

Xa = minimum wheel load

$$a = 1 - \Phi\left(\frac{\ell n Xa-\lambda}{\xi}\right)$$

The parameters of the respective distribution functions can be determined as follows.

For the exponential distribution, the parameter is

$$\lambda = 1/E[X]$$

in which, E[X] is the mean value of the data.

Applying the maximum likelihood method, the parameters of the normal tail distribution are determined by solving the following two equations numerically.

$$\frac{n}{(1-\Phi(\frac{Xa-\mu}{\sigma}))} \cdot f_N(\frac{Xa-\mu}{\sigma}) - \sum_{i=1}^{n} (\frac{Xi-\mu}{\sigma}) = 0 \tag{3.4}$$

$$n \left\{ \frac{1}{(1-\Phi(\frac{Xa-\mu}{\sigma}))} \cdot (\frac{Xa-\mu}{\sigma}) \cdot f_N(\frac{Xa-\mu}{\sigma}) - 1 \right\} + \sum_{i=1}^{n} (\frac{Xi-\mu}{\sigma})^2 = 0 \tag{3.5}$$

Similarly the parameters of the lognormal tail distribution are determined by solving the following two equations numerically.

$$\frac{n}{(1-\Phi(\frac{\ell nXa-\lambda}{\xi}))} \cdot f_N(\frac{\ell nXa-\lambda}{\xi}) - \sum_{i=1}^{n} (\frac{\ell nXi-\lambda}{\xi}) = 0 \tag{3.6}$$

$$n \left\{ \frac{1}{(1-\Phi(\frac{\ell nXa-\lambda}{\xi}))} \cdot (\frac{\ell nXa-\lambda}{\xi}) \cdot f_N(\frac{\ell nXa-\lambda}{\xi}) - 1 \right\} + \sum_{i=1}^{n} (\frac{\ell nXi-\lambda}{\xi})^2 = 0 \tag{3.7}$$

where:

$$f_N(x) = \frac{1}{\sqrt{2\pi}} \exp(-\frac{X^2}{2})$$

and n is the sample size

The results are summarized in Table 3.2

Table 3.2 ESTIMATED PARAMETERS OF DISTRIBUTIONS

Xa	Exponential (λ)	Gaussian Tail (μ)	(σ)	Lognormal Tail (λ)	(ξ)
4	1.5420	4.1428	1.8661	1.3729	0.3849
6	1.3110	6.1738	1.5612	1.7925	0.2338
8	1.2077	8.2103	1.4135	2.0868	0.1649

The cumulative probability of the instantaneous wheel load, therefore, are given by the following.

Exponential

with Xa = 4 F_{E4} =1-0.0495 EXP(-0.6485(X-4)) (3.8a)

with Xa = 6 F_{E6} =1-0.0136 EXP(-0.7628(X-6)) (3.8b)

with Xa = 8 $F_{E8} = 1 - 0.0028\ EXP(-0.8280(X-8))$ (3.8c)

Gaussian Tail

with Xa = 4 $F_{N4} = 0.9067 + 0.0933 \cdot \Phi(\frac{X-4.1428}{1.8661})$ (3.9a)

with Xa = 6 $F_{N6} = 0.9750 + 0.0250 \cdot \Phi(\frac{X-6.1738}{1.5612})$ (3.9b)

with Xa = 8 $F_{N8} = 0.9949 + 0.0051 \cdot \Phi(\frac{X-8.1465}{1.3690})$ (3.9c)

Lognormal Tail

with Xa = 4 $F_{L4} = 0.8982 + 0.1018 \cdot \Phi(\frac{\ell nX-1.3729}{0.3849})$ (3.10a)

with Xa = 6 $F_{L6} = 0.9728 + 0.0272 \cdot \Phi(\frac{\ell nX-1.7925}{0.2338})$ (3.10b)

with Xa = 8 $F_{L8} = 0.9946 + 0.0054 \cdot \Phi(\frac{\ell nX-2.0868}{0.1649})$ (3.10c)

These cumulative probabilities are plotted in Figs. 8, 9 and 10, together with the cumulative probabilities of the original data (as given in Table 3.1) above 4, 6 and 8 tons.

As shown in Fig. 3.1 the exponential distributions deviate considerably from the expirical distribution. Even the distribution F_{E8} overestimates the exceedance probabilities for wheel loads higher than 12 tons. Consequently, these exponential distributions are not appropriate for determining the lifetime maximum wheel load.

The normal tail distributions are shown in Fig. 3.2. Although the plot of the data on normal probability paper is not a straight line, the normal tail distributions follow the data behavior reasonably well. F_{N8} distribution, which seems to give the best fit among the distributions examined, is used in this report to estimate the lifetime maximum wheel load.

The lognormal tail distribution, as shown in Fig. 3.3, do not seem to fit the original data. Furthermore, the plot of the original data on lognormal probability paper does not give a straight line; these indicate that the lognormal type distributions are not appropriate to estimate the lifetime maximum wheel load.

From the above observations, it seems reasonable to model the distributions of the instantaneous wheel loads of heavy trucks with the F_{N8} distribution function. Results will also be derived with the F_{L8} distribution function, for the purpose of comparison.

By the theory of extreme valve statistics, the distribution function of the lifetime maximum wheel load is given by the following formula.
(Type-I Asymptotic)

$$F_I(X) = \exp\left\{ -e^{-\alpha(x-\mu)} \right\} \tag{3.11}$$

$$\mu_I = \mu + 0.577/\alpha$$

$$\sigma_I = \pi/\sqrt{6}\cdot\alpha$$

in which the parameters are;

u = the most probable lifetime maximum among N wheel load, which is equal to the value of the instantaneous wheel load at the cumulative probability of 1-1/N

N = the number of wheel loadings during the lifetime.

$\alpha = N\cdot f(u)$

The value of N depends on the location of a bridge, the kind of members and many other factors. In this study, results for N=100/day, 1000/day and 10,000/day are derived. A lifetime of 50/years is assumed.

The value of the parameters as well as the mean and standard deviation of the lifetime maximum wheel load are shown in Table 3.3. The mean lifetime maximum live load varies from 13 tons to 15 tons depending on the daily traffic volume. Observe that based on the lognormal tail distribution, the corresponding mean value varies from 15 tons to 18 tons.

It may be emphasized that the lifetime maximum wheel loads given in Table 3.3 do not include the effects of impact; such effects, of course, must be taken into consideration in the reliability analysis.

Table 3.3 LIFETIME MAXIMUM WHEEL LOAD

Traffic Volume	Distribution Function used	μ (tons)	α	μ (tons)	σ (tons)
100/day	F_{N8}	13.21	2.89	13.41	0.44
	F_{L8}	14.88	1.59	15.24	0.81
1000/day	F_{N8}	13.96	3.24	14.14	0.40
	F_{L8}	16.27	1.68	16.61	0.76
10000/day	F_{N8}	14.64	3.59	14.80	0.36
	F_{L8}	17.64	1.71	17.98	0.75

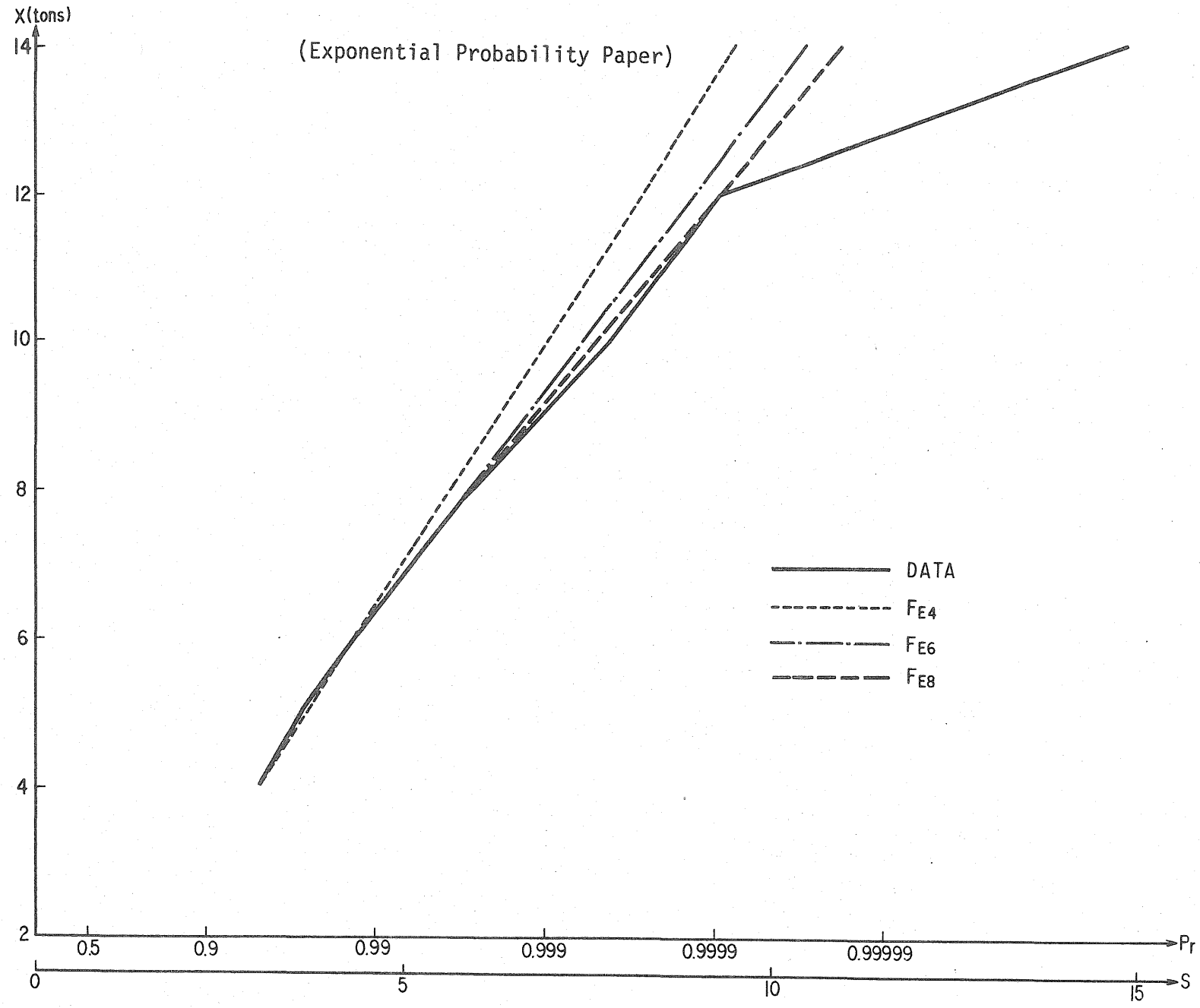

Fig. 3.1 ESTIMATION BY EXPONENTIAL DISTRIBUTION

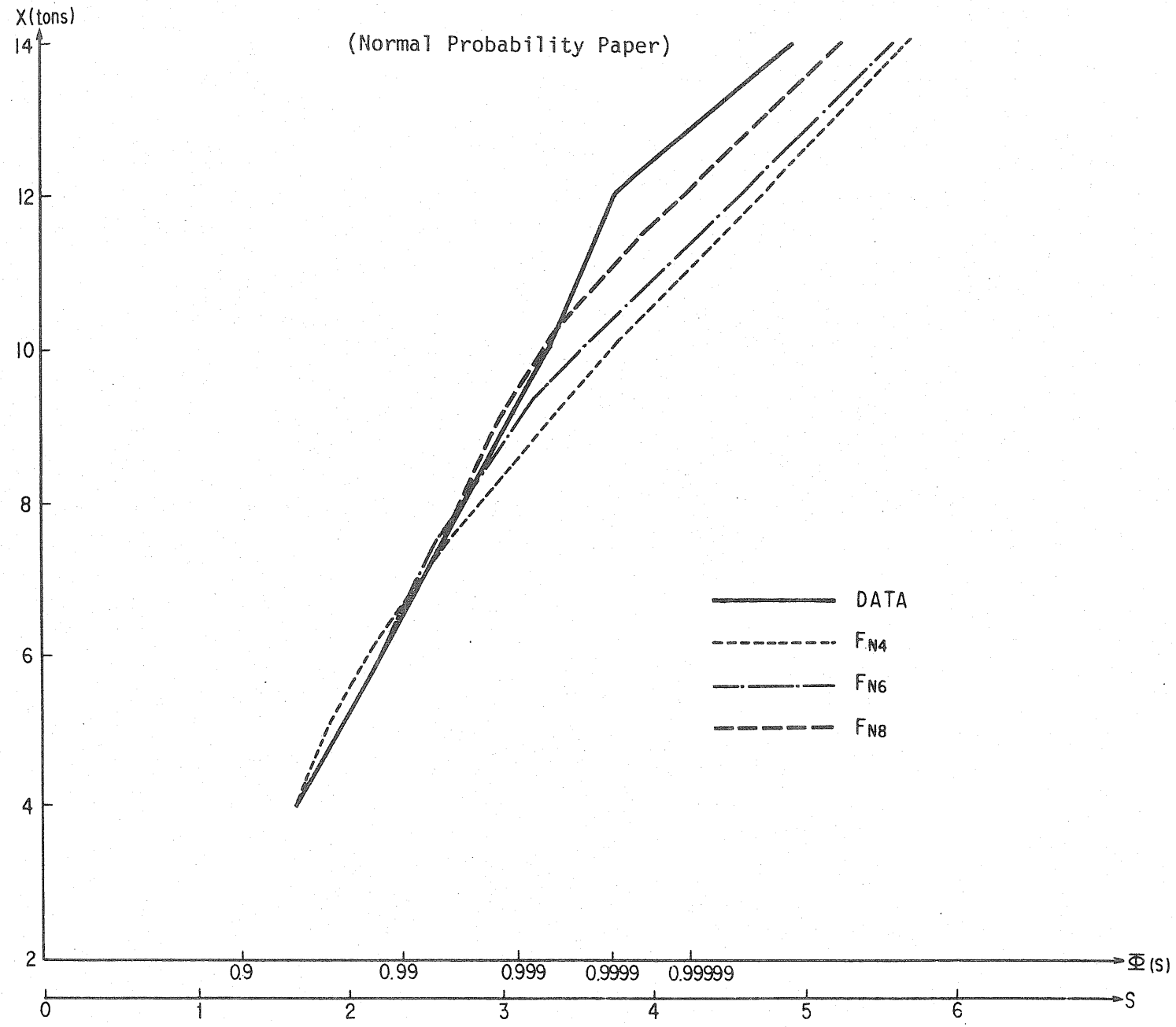

Fig. 3.2 ESTIMATION BY NORMAL TAIL

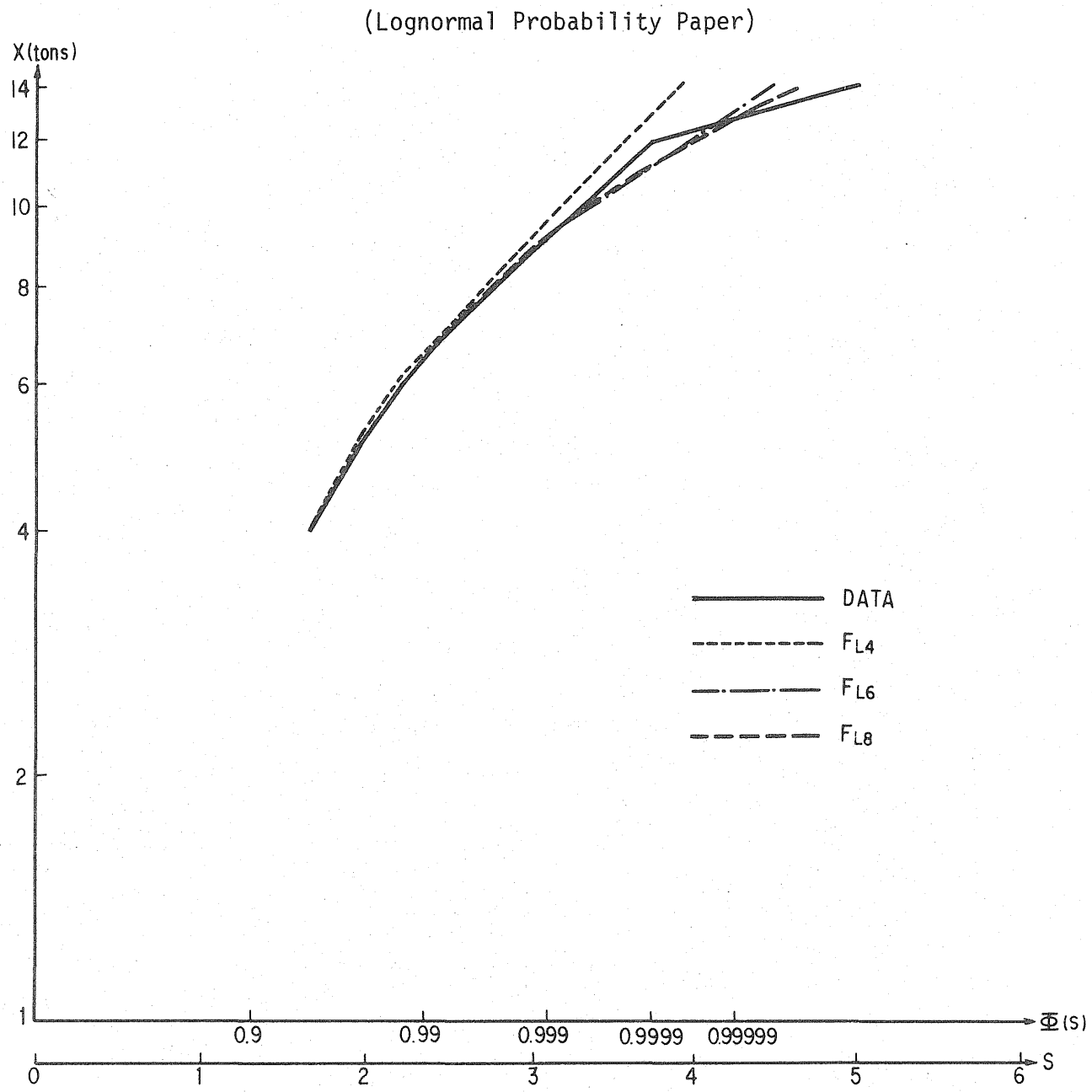

Fig. 3.3 ESTIMATION BY LOGNORMAL TAIL

3.2 Live Load on Long-Span Bridges

Live load on long span bridges is determined by a line of vehicles. For design purposes, equivalent uniformly distributed load or concentrated load is specified in specifications. For example, Specifications for Highway bridges in Japan (1973) specify the following design live load.

P = concentrated load at a critical section (5000kg/m)

q = uniformly distributed load of

$350kg/m^2$	for span $\leq$ 80m
$430-span(m)kg/m^2$	for 80m < span < 130m
$300kg/m^2$	for 130m $\leq$ span

Such code specified live load may be much smaller than the load caused by a long line of heavy vehicles, because the design live load is reduced for long-span bridges based implicitly on probability concepts. The adequacy of such design live loads should be examined based on actual traffic conditions.

Computer simulations were performed to determine the distribution of the maximum bending moment and shear due to jammed traffic loads. The simulations were based on data collected from Japanese bridges as follows.

1. Several congested points on the Japanese national highways were chosen, and cameras were set in tall buildings near by.
2. Pictures were taken continuously for each point.
3. From the pictures, dimensions of each vehicle were determined. On the basis of the dimensions and the load condition of each vehicle, the vehicles were classified into categories shown in Table 3.4.
4. Finally, the proportion (in percent) of each category of vehicles was determined as summarized in Table 3.5.

It may be well to emphasize that the data were collected under the following conditions: The category of each vehicle is determined from the pictures, on the basis of which the weight of each vehicle is assigned. The cameras were set up at measuring points where the rate of heavy trucks and overall traffic volume are the highest among the national highways near Tokyo. Finally, the data were obtained at night, when the rate of heavy trucks is the highest. So, the results may be applied to the national highways where traffic conditions are the severest.

The simulations were performed based on the following assumptions.

1. The severest loading condition is that of a completely jammed traffic condition, even though there is no impact under a jammed condition. In a completely jammed condition, the distance between adjacent cars has been found to be 1.0m. (P.W.R.I. 1974, P.W.R.I. 1971)
2. There is no correlation between the categories of adjacent vehicles, the rate of which are shown in Table 3.5.
3. The dimensions and weight of vehicles shown in Table 3.4 contain uncertainty, expressed in terms of C.O.V. around the mean value shown in Table 3.4.
4. The width of a lane is 3.5m.

The computer simulations were performed assuming the values of the parameters shown in Table 3.6; these are chosen to examine the variance of the live load due to location, span, error in modeling and so on. The simulated live loads are divided by the design live loads, and are shown in Table 3.6 and also in Figures 3.4 through 3.6.

Fig. 3.4 a and b show the distributions of the live loads for the various locations indicated in Table 3.6. In Fig. 3.4 a, the results are plotted on normal probability paper, whereas Fig. 3.4 b shows the same results plotted on lognormal probability paper. The variance of the live loads due to locations is quite large. However, irrespective of locations, the lognormal distributions appear to be a better model of the simulated live loads, on the basis of the linearity of the plots.

Fig. 3.5 shows the live loads on various span lengths. It appears that the live loads on long span bridges are about the same as those on short span bridges in comparison to the design live loads. However, the C.O.V. in the live loads becomes smaller as the span gets longer. This fact (i.e. higher live load uncertainty in short span bridges) should be reflected in the determination of load factors; higher load factors should be expected for short span bridges.

Fig. 3.6 shows that larger uncertainty in the dimensions and in the weight of vehicles (Ω_D and Ω_W in Table 3.6) increases the variance of the simulated result. It is difficult to estimate the uncertainty exactly, but Ω_D=0.1 and Ω_W=0.2 would be reasonable to cover the imperfection of the simulation model and sampling.

Table 3.4 CATEGORY OF VEHICLES

Category #	Classification	Dimensions (Width-length)	No. of Axles	Loaded or Empty	Weight(tons)
1	Light Vehicles	1.5 - 3.0	2	-	1.0
2	Passenger cars	1.5 - 4.0	2	-	1.0
3	Trucks	2.0 - 5.0	2	Empty	2.0
4	Trucks	2.0 - 5.0	2	Loaded	4.0
5	Trucks	2.0 - 6.0	2	Empty	3.5
6	Trucks	2.0 - 6.0	2	Loaded	7.5
7	Trucks	2.5 - 7.0	2	Empty	5.0
8	Trucks	2.5 - 7.0	2	Loaded	11.0
9	Trucks	2.5 - 7.5	2	Empty	6.0
10	Trucks	2.5 - 7.5	2	Loaded	14.5
11	Trucks	2.5 - 9.0	2 or 3	Empty	8.0
12	Trucks	2.5 - 9.0	2 or 3	Loaded	18.0
13	Trailers	2.5 -15.0	3 or 4	Empty	11.0
14	Trailers	2.5 -15.0	3 or 4	Loaded	27.0
15	Buses	2.0 - 6.0	2	-	4.0
16	Buses	2.5 -10.0	2 or 3	-	10.0

Table 3.5 PROPORTION OF EACH CATEGORY OF VEHICLES (%)

Cat. #	Point #1 Ohmori	Point #2 Ohhara	Point #3 Abiko	Point #4 Utsunomiya	Point #5 Shimizu
1	2.3	1.9	2.0	0.3	0.5
2	46.1	25.9	29.9	12.7	10.4
3	3.1	5.6	4.0	2.7	1.6
4	10.2	7.4	4.7	4.5	1.3
5	2.7	3.4	.8	1.7	0.5
6	5.1	7.9	11.6	6.9	8.3
7	1.6	3.3	1.6	2.0	0.0
8	3.9	10.4	5.8	11.7	11.5
9	0.8	1.3	1.6	1.7	1.1
10	3.5	4.4	6.4	7.3	3.8
11	1.6	4.5	6.0	3.0	2.7
12	18.7	20.9	20.3	43.6	53.6
13	0.0	0.3	0.0	0.3	0.0
14	0.4	0.8	3.8	0.9	4.3
15	0.0	1.9	0.0	0.2	0.4
16	0.0	0.2	0.4	0.3	0.0

(% of total occurrences)

Table 3.6 TYPICAL RESULTS OF SIMULATION

Simulation Case #	Point # (Table 7)	Span	Ω_D	Ω_W	Sample Size	μ	σ
1	1	80.0	0.1	0.2	200	0.740	0.219
2	2	80.0	0.1	0.2	200	0.866	0.194
3	3	80.0	0.1	0.2	200	0.899	0.201
4	4	80.0	0.1	0.2	200	1.121	0.180
5	5	80.0	0.1	0.2	200	1.216	0.184
6	5	40.0	0.1	0.2	200	1.197	0.243
7	4	120.0	0.1	0.2	200	1.278	0.156
8	5	120.0	0.1	0.2	200	1.377	0.161
9	5	80.0	0.1	0.1	200	1.214	0.148
10	5	80.0	0.1	0.3	200	1.218	0.227
11	5	80.0	0.1	0.2	500	1.215	0.179

Ω_D, Ω_W = The C.O.V. of dimensions and weight of vehicles

μ, σ = The mean and standard deviation of the simulated live load intens
intensity divided by the design live load intensity

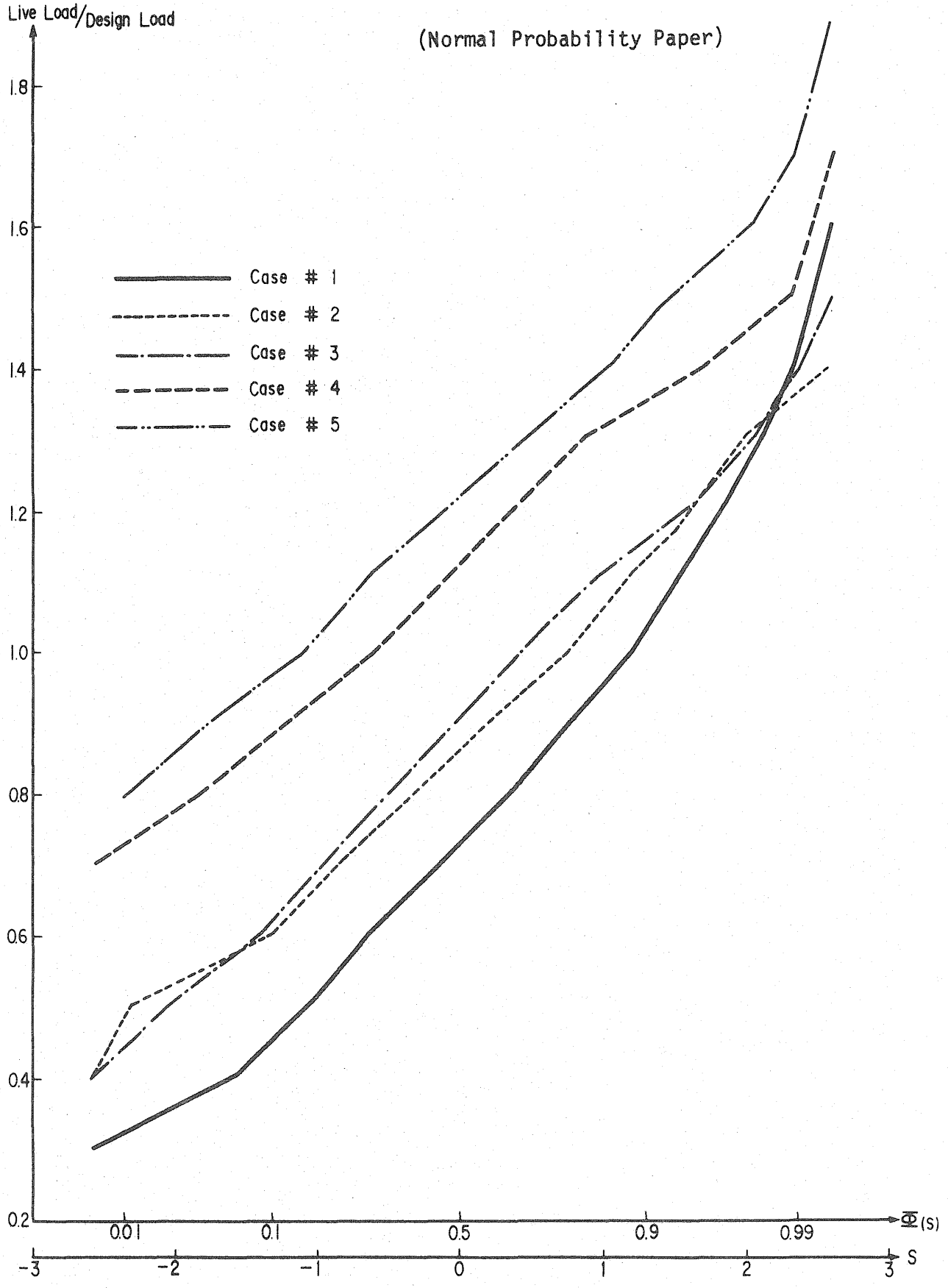

Fig. 3.4(a) SIMULATED LIVE LOAD (SPAN = 80m)

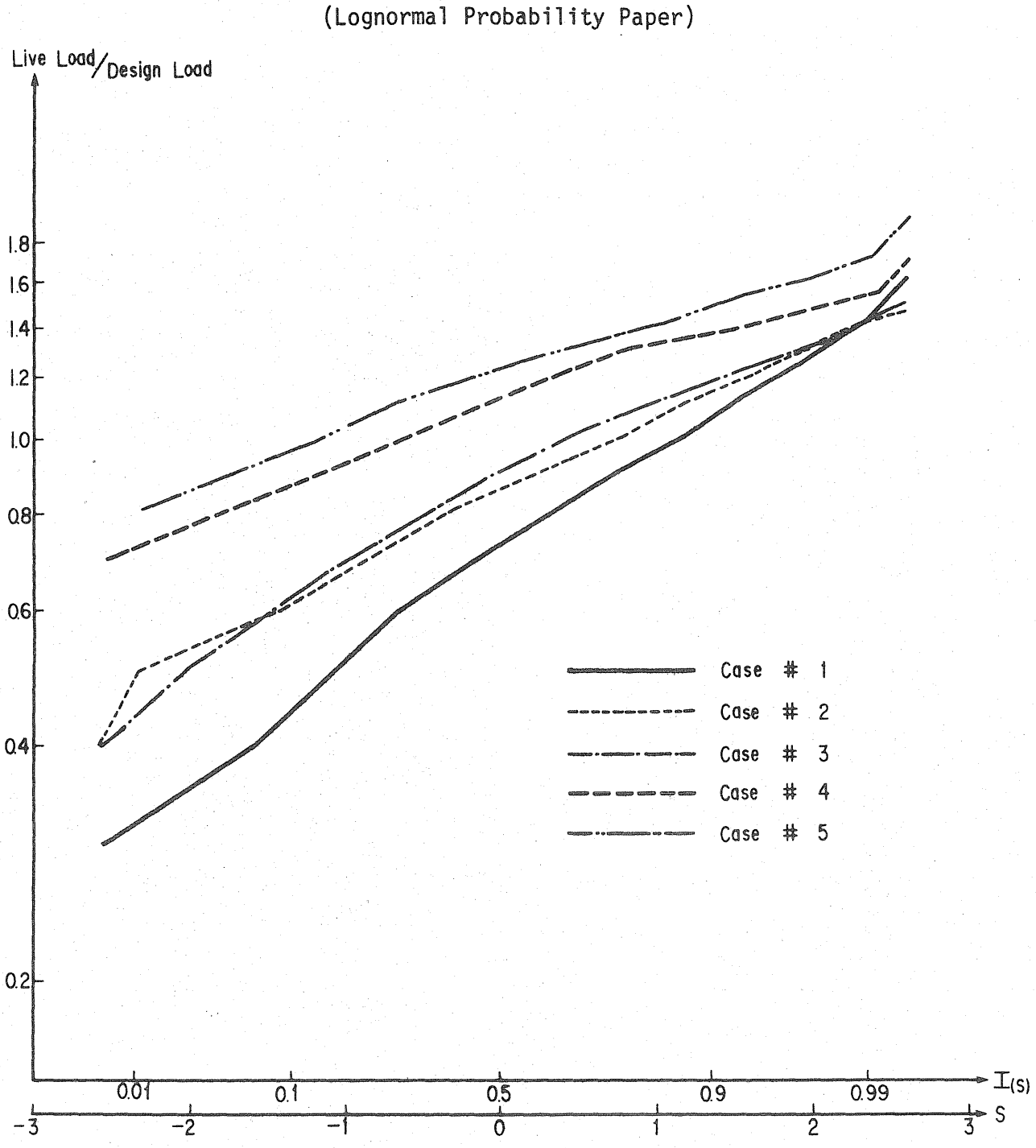

Fig. 3.4(b) SIMULATED LIVE LOAD (SPAN = 80m)

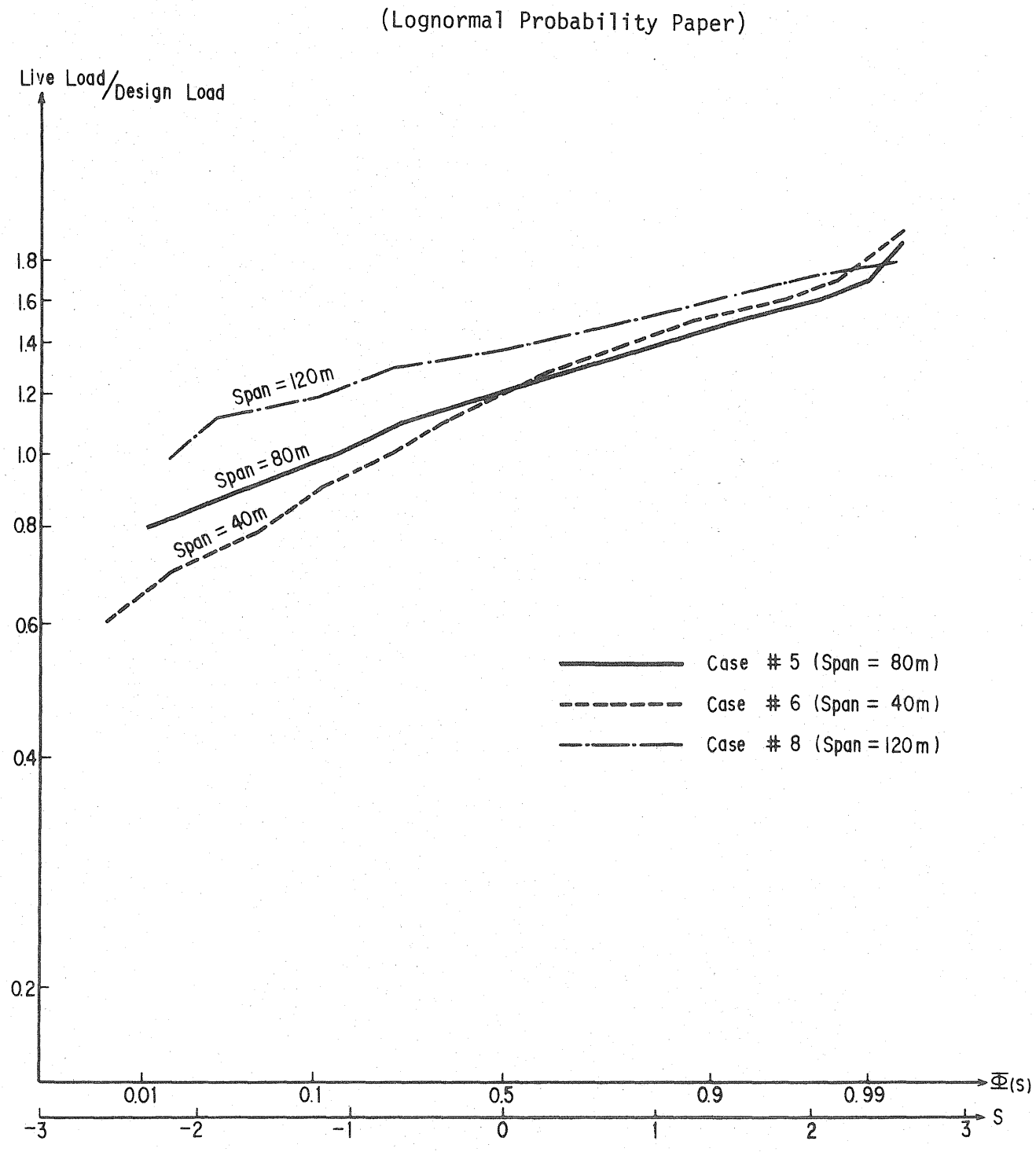

Fig. 3.5 SIMULATED LIVE LOAD FOR VARIOUS SPAN LENGTHS

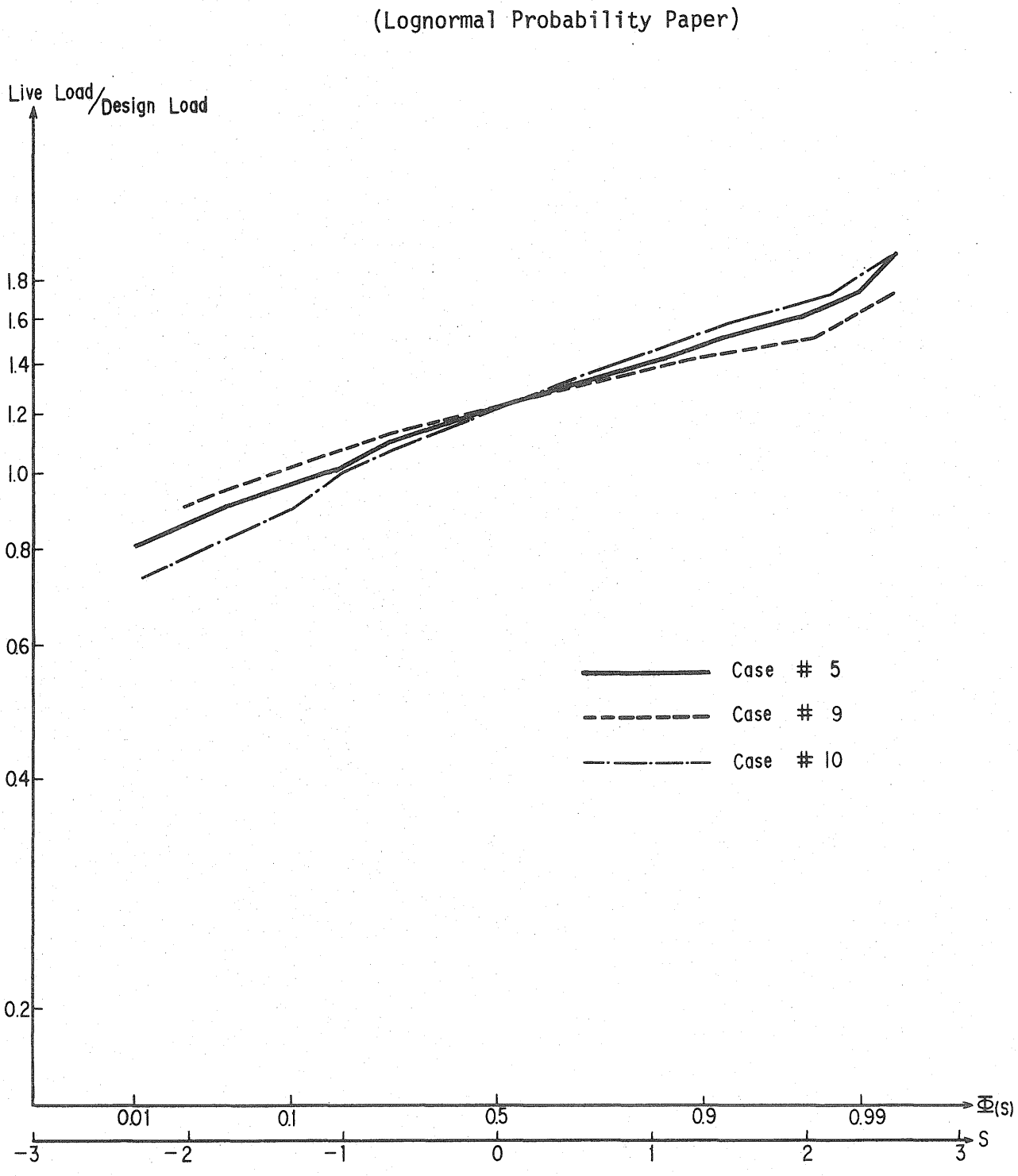

Fig. 3.6 EFFECT OF C.O.V. ON SIMULATED LIVE LOAD

The sample size used in the computer simulation is limited to 200. From the results shown in Table 3.6, a sample size of 200 appears to give reasonably accurate results, e.g. comparing Case #5 and 11.

The above simulated live loads may be used to determine the lifetime maximum live load. For this purpose, Point #5 is chosen to represent the severe conditions on national highways. From Table 3.6, the mean and C.O.V. of the simulated results and the corresponding parameters of the lognormal distributions at Point #5 are given as follows.

Table 3.7 SIMULATED LIVE LOAD AT POINT #5

Span(m)	μ	Ω	λ	ξ
40	1.197	0.203	0.160	0.201
80	1.216	0.151	0.184	0.150
120	1.377	0.117	0.313	0.117

The parameters shown above contain the uncertainty due to model imperfection a reflected in Ω_D and Ω_W. However these should be augmented by the uncertainty in the width of a lane. In this regard, a C.O.V. of 10% is added. So, the mean and C.O.V. and the parameters of the lognormal distributions to be used in determining the lifetime maximum live load are as follows.

Table 3.8 MODIFIED LIVE LOAD AT POINT #5

Span(m)	μ	Ω	λ	ξ
40	1.197	0.226	0.155	0.223
80	1.216	0.181	0.179	0.180
120	1.377	0.154	0.308	0.153

The 50 year lifetime maximum live load will depend on the number of times that completely jammed conditions will occur during the night. Assuming that completely jammed condition oocurs at average rate of 0.1, 1 and 10 times daily, the lifetime maximum live loads would be obtained as follows.

Table 3.9 LIFETIME MAXIMUM LIVE LOAD

Span(m)	0.1 time daily		1 time daily		10 times daily	
	μ	σ	μ	σ	μ	σ
40	2.503	0.193	2.855	0.194	3.192	0.187
80	2.213	0.139	2.461	0.136	2.694	0.128
120	2.296	0.123	2.513	0.119	2.713	0.110

No impact load is expected in a completely jammed condition, whereas in the design of box girder bridges impact loads are always taken into consideration. The values shown in Table 3.9, therefore, should be reduced, making allowance for the impact load. On this basis, the reduced lifetime maximum live load is given by the following.

Table 3.10 MODIFIED LIFETIME MAXIMUM LIVE LOAD

Span(m)	0.1 time daily		1 time daily		10 times daily	
	μ	σ	μ	σ	μ	σ
40	2.048	0.193	2.336	0.194	2.612	0.187
80	1.919	0.139	2.134	0.136	2.316	0.128
120	2.054	0.123	2.248	0.119	2.427	0.110

It is reasonable to expect that the number of times of completely jammed condition will be higher for short span bridges than for long span bridges. Accordingly, the mean lifetime maximum live loads on short span bridges should be higher than those for long span bridges; moreover, the uncertainty in the short span live load is larger than that of long span bridges. These ought to be reflected in the specifications of design live loads, in order to maintain consistent levels of safety for different span lengths.

3.3 Earthquake

For design, or safety analysis purposes, the maximum earthquake ground acceleration over the lifetime of a structure is of interest. The maximum ground motion during an earthquake depends on many factors, including the rock strata, existence of faults, proximity of a site to a fault break, and so on.

In this study, the ground acceleration in downtown Tokyo (E39.8, N35.7), where the natural period of the ground is 0.3 seconds, is analysed.

Table 3.11 shows the annual maximum ground acceleration in Tokyo on the site where the natural period of the ground is 0.3 seconds. This set of data (Hattori 1977) was obtained using statistical data on the magnitude and on the epicentral distances of earthquakes since 1926 and converting them into the maximum acceleration by Kanai's spectrum (Kanai 1968). The maximum acceleration during 47 years is 157.93 cm/s^2, which was recorded in the famous Kanto Earthquake of 1931.

To calculate the theoretical maximum ground acceleration during the lifetime of a structure, a distribution function suitable for the annual maximum acceleration shown in Table 3.11 must be obtained. In this regard, the Type I or Type II asymptotic distribution is theoretically reasonable, because the data in Table 3.11 are extreme values. The Type I and Type II extreme value distribution functions are given as follows.

$$F_I(X) = \exp\left\{ -e^{-\alpha(x-\mu)} \right\} \tag{3.12}$$

$$F_{II}(X) = \exp\left\{ -\left(\frac{V}{X}\right)^K \right\} \tag{3.13}$$

where μ, α, V and K are parameters.

The value of the parameters can be estimated by using the first and second moments of the data shown in Table 3.11. On this basis the parameters μ, α, V and K are estimated to be as follows.

Type I ; μ=18.19 α=0.0429

Type II; V=15.30 K=1.530 (in cm/s^2)

The data and the Type I and Type II distributions estimated above are plotted in Fig. 3.7 on Gumbel probability paper. From the plots on this figure, it is evident that the Type I distribution will underestimate the maximum acceleration during the lifetime of a structure. The Type II distribution seems to give reasonable fit with the original data, including the Kanto earthquake. In this report, therefore, the Type II distribution was adopted to analyse the risk due to earthquakes, that is, the annual maximum acceleration due to earthquakes is given by the following distribution.

$$FII(X) = \exp\left\{ -\left(\frac{15.3}{X}\right) \right\}^{1.53} \quad \text{(unit cm/s}^2\text{)} \tag{3.14}$$

In the design of bridges, vertical acceleration due to earthquake is of small importance, although it is sometimes important in the design of building structures. In the design of bridges, the dead weight of superstructures is not so large except for very long-span bridges. So, even if the vertical seismic coefficient is 0.1, the total vertical load intensity will only increase slightly. Moreover in the design of the substructures, the bending moment induced by the horizontal acceleration is dominant. So, in this report, vertical acceleration is not examined.

Table 3.11 ANNUAL MAXIMUM GROUND ACCELERATION IN TOKYO (HATTORI 1977)

(Natural Period of the ground = 0.3 second)

A.D.	Epicentral Distance(Km)	Richter Magnitude	Acceleration (cm/s^2)	A.D.	Epicentral Distance(Km)	Richter Magnitude	Acceleration (cm/s^2)
1926	48.10	6.2	89.75	1950	84.96	6.5	61.18
1927	141.66	6.0	14.08	1951	58.60	6.2	68.36
1928	76.10	5.8	26.87	1952	104.41	5.5	11.07
1929	70.30	6.1	45.91	1953	226.82	6.6	15.76
1930	98.28	7.0	99.61	1954	126.80	6.4	29.25
1931	71.71	7.0	157.93	1955	74.33	5.3	13.77
1932	120.89	6.1	20.63	1956	50.82	6.0	62.88
1933	114.21	5.6	11.14	1957	155.63	5.0	2.99
1934	58.86	5.2	16.68	1958	43.95	4.4	8.09
1935	149.20	6.3	19.83	1959	123.03	5.6	9.95
1936	142.85	6.3	21.19	1960	177.37	5.9	8.66
1937	119.98	6.6	42.12	1961	147.25	5.9	11.53
1938	113.99	6.6	35.62	1962	79.25	4.9	7.16
1939	67.22	5.3	15.91	1963	136.45	6.1	17.16
1940	117.23	6.1	21.47	1964	132.40	6.2	20.68
1941	75.36	6.0	36.09	1965	152.50	6.7	33.62
1942	141.15	6.6	32.90	1966	57.10	4.9	11.42
1943	151.62	6.6	29.48	1967	87.38	5.6	16.04
1944	23.50	5.5	82.90	1968	70.10	6.1	46.09
1945	68.01	5.7	27.44	1969	65.84	4.5	5.33
1946	71.17	6.3	59.73	1970	84.05	5.1	8.70
1947	118.30	6.0	18.52	1971	70.85	4.9	8.41
1948	74.03	5.4	15.94	1972	58.60	5.1	14.58
1949	114.38	6.7	52.90				

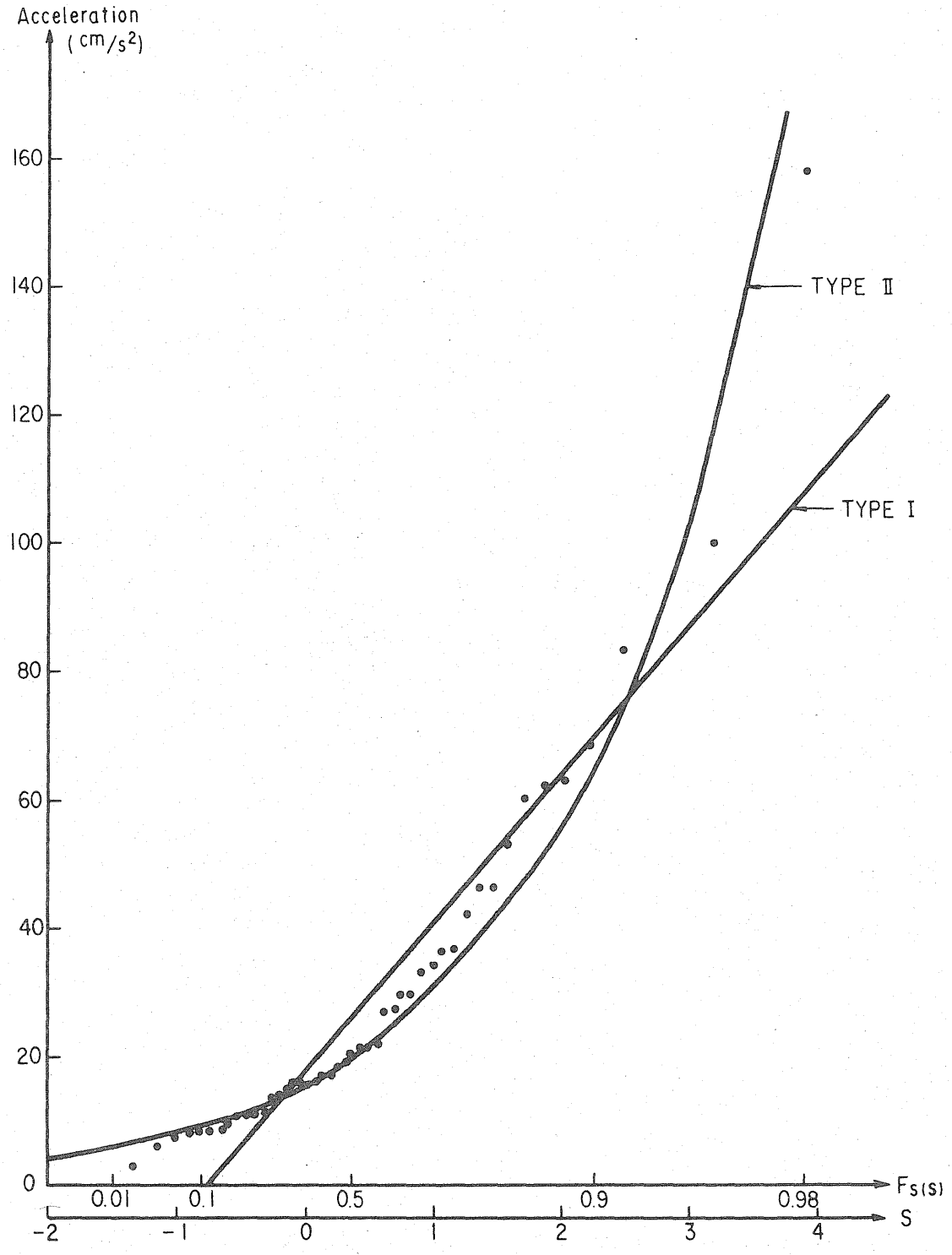

Fig. 3.7 PLOTS ON GUMBEL PROBABILITY PAPER

CHAPTER 4

RELIABILITY ANALYSIS OF BOX GIRDER BRIDGES IN JAPAN

4.1 Basic Theory

The first-order second moment reliability analysis is adopted to evaluate the reliability of box girder bridges in Japan. Many research works have been made on the first-order second moment reliability analysis (for example, Ang 1976). The outline of the theory is summarized here.

The resistance R and the lifetime maximum load S are, respectively, functions of basic resistance and load variables. That is,

$$R = g_R\ (R_1,\ R_2,\ \text{-----},\ R_n)$$
$$S = g_S\ (S_1,\ S_2,\ \text{-----},\ S_n) \tag{4.1}$$

From which we obtain,

$$\mu_R \cong \bar{v}_{gR} \cdot \hat{g}_R\ (\mu_{R1},\ \mu_{R2},\ \text{-----},\ \mu_{Rn})$$
$$\mu_S \cong \bar{v}_{gs} \cdot \hat{g}_s\ (\mu_{S1},\ \mu_{S2},\ \text{-----},\ \mu_{Sn}) \tag{4.2}$$

and

$$\Omega_R^2 \cong \Omega_{gR}^2 + \frac{1}{\mu R^2} \Sigma\Sigma\ Pij \cdot Ci \cdot Cj \cdot \sigma_{Ri} \cdot \sigma_{Rj}$$
$$\Omega_S^2 \cong \Omega_{gs}^2 + \frac{1}{\mu s^2} \Sigma\Sigma\ Pij \cdot Ci \cdot Cj \cdot \sigma si \cdot \sigma sj \tag{4.3}$$

where,

μR, μS = mean value of the resistance R and the load S

ΩR, ΩS = C.O.V. of the resistance R and the load S

$\bar{v}_{gR}$, $\bar{v}_{gs}$ = mean bias in the functions $\hat{g}_R$ and $\hat{g}_s$

Ω_{gR}, Ω_{gs} = C.O.V. of the bias in the functions $\hat{g}_R$ and $\hat{g}_s$

g_R, g_s = idealized functions of g_R and g_s

Pij = correlation coefficient between the i-th and j-th variable

Ci = $\partial g / \partial xi$

Subsequently, the following performance function and limit state are assumed.

$$Z = \ell n\ R/S$$

$$z_o = 0$$

Then prescribing Z to be normal, the probability of failure of the structure is

$$P_F = 1 - \Phi\left(\frac{\ell n(R/S)}{\sqrt{\Omega R^2 + \Omega S^2}}\right) \tag{4.4}$$

where $\Phi(x)$ is the cumulative probability of the standard Gaussian distribution.

In design specifications, the total safety factor can be given by the following, based on the second moment reliability theory.

$$\theta^* \geq \frac{CR}{CS} \cdot \frac{\nu S}{\nu R} \cdot e^{\beta\Omega} \tag{4.5}$$

in which,

θ^* = total safety factor

CR, CS = the ratio of the nominal design values to the mean values of R and S

νR, νS = the mean biases in the estimated mean values of R and S

$\Omega = \sqrt{\Omega S^2 + \Omega R^2}$

$\beta = \phi^{-1}(1-P_F)$, the safety index

Design to achieve a desired reliability may also be accomplished using resistance and load factor. In this case, the design criterion is given by

$$\phi^* \cdot R^* \geq \gamma^* \cdot S^* \tag{4.6}$$

where, ϕ^* and γ^* is given by

$$\left.\begin{aligned} \phi^* &= \frac{\nu R}{CR}\ e^{-0.75\cdot\beta\cdot\Omega R} \\ \gamma^* &= \frac{\nu S}{CS}\ e^{0.75\cdot\beta\cdot\Omega Q} \end{aligned}\right\} \tag{4.7}$$

To reflect the different uncertainties in the loading, multiple load factor design format is sometimes convenient, in which the design format becomes

$$\phi^*\cdot R^* \geq \gamma_1^*\cdot S_1^* + \gamma_2^*\cdot S_2^* + \text{---} + \gamma_n^*\ S_n^* \tag{4.8}$$

where the load factors are determined by first determining α by trial and error through the following:

$$(\bar{S}_1 + \bar{S}_2 + \cdots + \bar{S}n)\, e^{0.75\cdot\beta\cdot\Omega S}$$

$$= \bar{S}_1 \cdot e^{0.75\alpha\cdot\beta\cdot\Omega S_1} + \bar{S}_2 \cdot e^{0.75\alpha\cdot\beta\cdot\Omega S_2} + \cdots + \bar{S}n \cdot e^{0.75\alpha\cdot\beta\cdot\Omega Sn} \qquad (4.9)$$

The load factors are then,

$$\gamma i^* = \frac{\nu S}{CS}\, e^{0.75\cdot\alpha\cdot\beta\cdot\Omega Si} \qquad (4.10)$$

4.2 Reliability of Box Girders

The box girder bridges examined here are standard simply-supported single span bridges with reinforced concrete slabs. The spans of the bridges are 40, 80 and 120 meters. The cross section of a typical box girder bridge is shown in Fig. 4.1 with the corresponding design conditions.

The box girder bridges examined here are designed to resist dead load, live load including impact, and earthquake load in accordance with the Specifications for Highway Bridges in Japan 1973. As discussed earlier, the vertical acceleration due to earthquake is of no importance in the design of bridge superstructures.

The nominal design stress is specified to be 1400kg/cm^2 for both R_R=0.5 and R_R=0.7 for box girder bridges composed of SS41 mild structural steel. In this report, the dimensions of box girder bridges are determined by computer programs so that the design stresses are less than but close to 1400kg/cm^2. The probability of failure is calculated based on the first-order second moment reliability theory summarized in Sect. 4.1.

The information needed in the reliability analysis is as follows.

1) Resistance

Ultimate strength (Sect. 2.3)

R_R = 0.5 $\quad \sigma cr/\sigma y$ = 0.982 $\quad \Omega$ = 0.059

R_R = 0.7 $\quad \sigma cr/\sigma y$ = 0.854 $\quad \Omega$ = 0.068

Serviceability (Sect. 2.3)

R_R = 0.5 $\quad \sigma cr/\sigma y$ = 0.723 $\quad \Omega$ = 0.108

R_R = 0.7 $\quad \sigma cr/\sigma y$ = 0.592 $\quad \Omega$ = 0.132

where σcr is the limit state stress and σy is the yield point stress of the material. Ω is the total C.O.V.

Section modulus and yield point (P.W.R.I. 1977)

The value of the actual limit state stress divided by the nominal limit state stress is slightly higher than 1.0, because conservative values of the section modulus and yield point stress are nominally specified. For structures composed of mild steel, the mean and the C.O.V. of this is

$\mu = 1.180$ $\Omega = 0.069$

2) Load Intensity

Dead load (P.W.R.I. 1977)

The ratios of the actual load intensity to the design load intensity for the dead weight of concrete slabs and steel members are as follows.

concrete slabs	$\mu = 1.032$	$\Omega = 0.060$
steel members	$\mu = 1.010$	$\Omega = 0.018$

Live load (Sect. 3.2)

Information on live loads are shown in Table 3.10.

3) Analysis

A C.O.V. of 5% is assumed for possible errors in the structural analysis of box girder bridges.

With the information given above, the probabilities of service failure and ultimate failure over a lifetime of 50 years are calculated. The results are summarized in Fig. 4.2. These are based on the assumption that completely jammed traffic condition on the bridge occurs 0.1 times daily.

Again, it must be emphasized that the failure here refers to the occurrence of buckling of box girders as defined in Fig. 2.3. The occurrence of the buckling may not necessarily mean collapse. However, the probabilities shown in Fig. 4.2 are reasonable measure of safety.

From Fig. 4.2, it can be seen that short-span bridges on major national highways in Japan may have unacceptable safety level. The lifetime maximum load will easily exceed the serviceability limit state, and sometimes even the ultimate limit state. In contrast, long span bridges may be sufficiently safe, especially if they are designed with R_R=0.5. However, there is a high probability that the lifetime maximum load will exceed the limit state of serviceability even in long-span bridges.

On the basis of the results obtained above, the following observations may be made.

1. The safety of bridges designed according to the current specifications in Japan varies with the span.
2. The probability of failure for ultimate strength is generally too high; especially for short-span bridges.
3. The lifetime maximum load will likely exceed the serviceability limit, which could cause problems in the rigidity or out-of-plane deflections of bridges.
4. The reliability of box girder bridges depends on the equivalent breadth-to-thickness ratio of girder flanges. Design of girders with R_R=0.7 will result in unacceptable safety level.

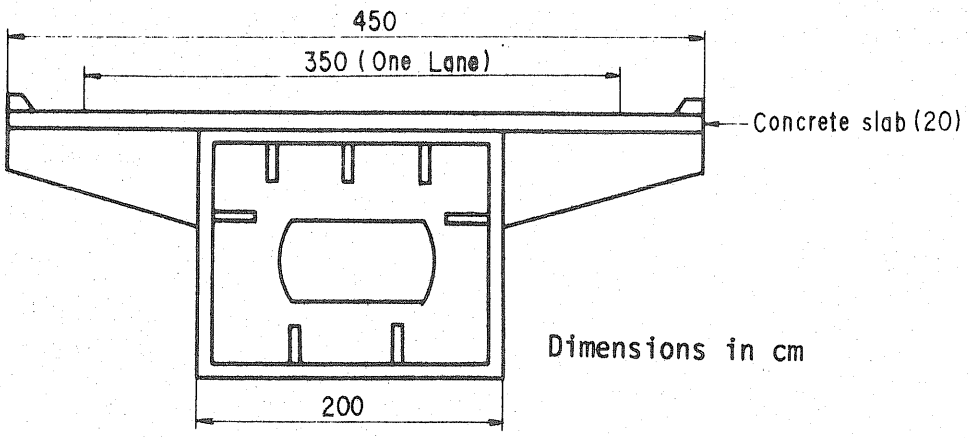

Fig. 4.1 CROSS SECTION OF TYPICAL BOX GIRDER BRIDGE

DESIGN CONDITIONS

Span = 40, 80, 120m
Simply-supported single span box girder bridge
Height of girders = span/25.0
Thickness of concrete slab = 20cm
Equivalent breadth-to-thickness ratio = 0.5 and 0.7
Width of a lane = 3.5m
Width of a slab = 4.5m
Width of a box girder = 2.0m
Material : SS41
Specifications : Specifications for Highway Bridges in Japan

(Frequency of completely jammed condition = 0.1 time daily)

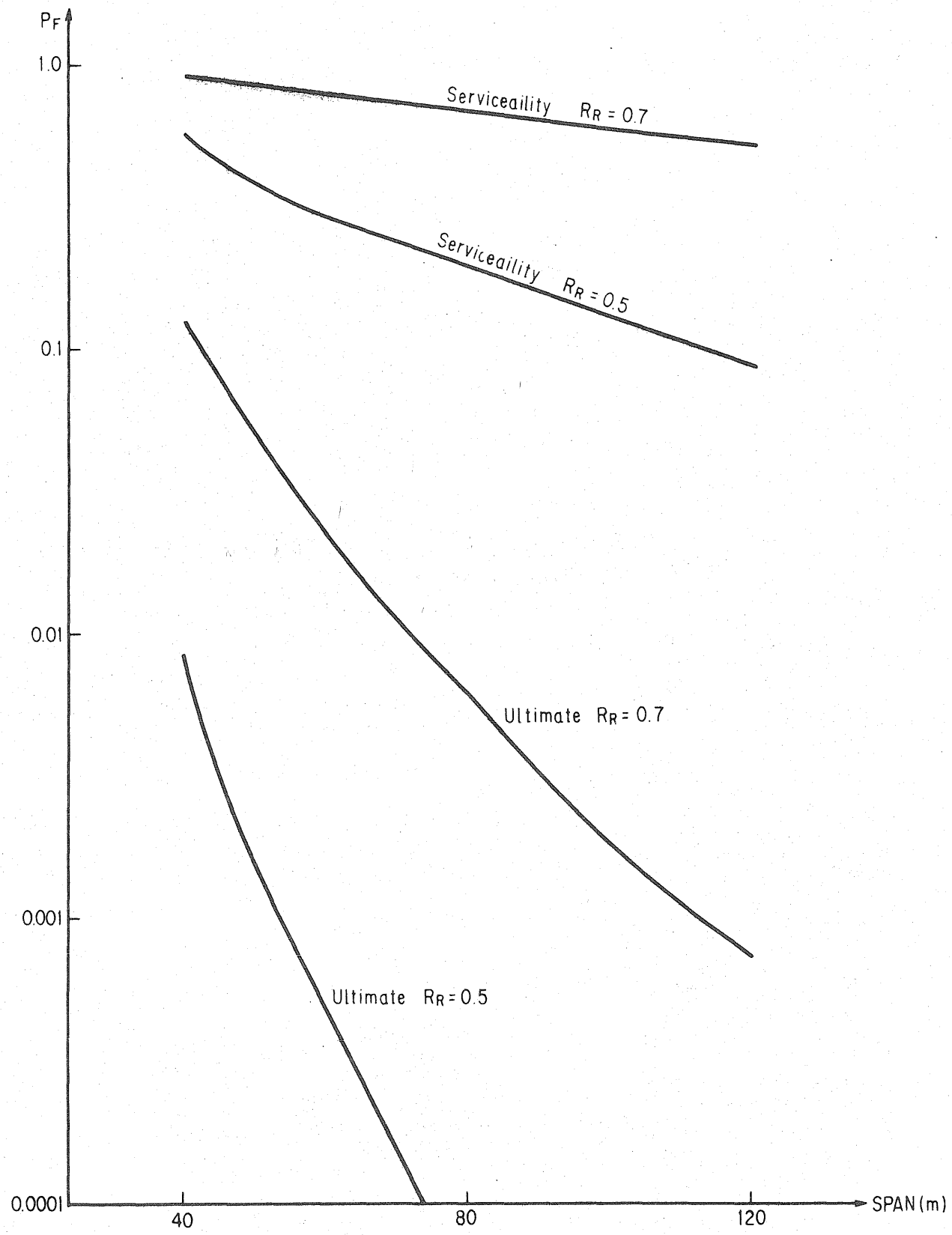

Fig. 4.2 PROBABILITY OF FAILURE OF BOX GIRDER BRIDGES

4.3 Reliability-Based Design Requirements for Box Girders

Part of the problem arises from the fact that the present code specifies the same safety factors for dead load and live load. The use of load factor design method may lead to more consistent levels of safety. In this report, the resistance factors and load factors for the design of box girders are developed, using the information obtained above and the second moment reliability analysis described in Sect. 4.1.

First, the nominal resistance of box girders may be determined as follows based on the results in Sect. 2.3.

Ultimate Limit $U^* = -0.920R_R + 0.277R_R^2 - 0.046R_R^3 + 1.378$ (4.1)

Serviceability Limit $S^* = -1.587R_R + 1.022R_R^2 - 0.267R_R^3 + 1.294$ (4.2)

for $\gamma = \gamma^*$

Resistance factors and load factors can be obtained, applying the theory shown in Sect. 4.1. In this report, β=3.0 (probability of failure around 0.0015) is assumed for the ultimate limit state, and β=2.0 (probability of failure around 0.025) is assumed for the serviceability limit state. Values of these factors depend on the spans and breadth-to-thickness ratio as follows.

Resistance factors (including the variance due to analysis error)

Ultimate limit	R_R=0.5	Ψ=0.962
	R_R=0.7	Ψ=0.949
Serviceability limit	R_R=0.5	Ψ=0.974
	R_R=0.7	Ψ=0.944

Load factors

For span = 40m:	Ultimate	-- 1.125 D + 2.451 L
	Serviceability	-- 1.089 D + 2.309 L
For span = 80m:	Ultimate	-- 1.125 D + 2.225 L
	Serviceability	-- 1.089 D + 2.118 L
For span =120m:	Ultimate	-- 1.125 D + 2.343 L
	Serviceability	-- 1.089 D + 2.243 L

For convenience in design, the following sets of resistance and load factors may be used for all spans and breadth-to-thickness ratios,

For Ultimate : $0.95\ R \geq 1.15\ D + 2.30\ L$ (4.3)

For Serviceability: $0.95\ R \geq 1.10\ D + 2.20\ L$ (4.4)

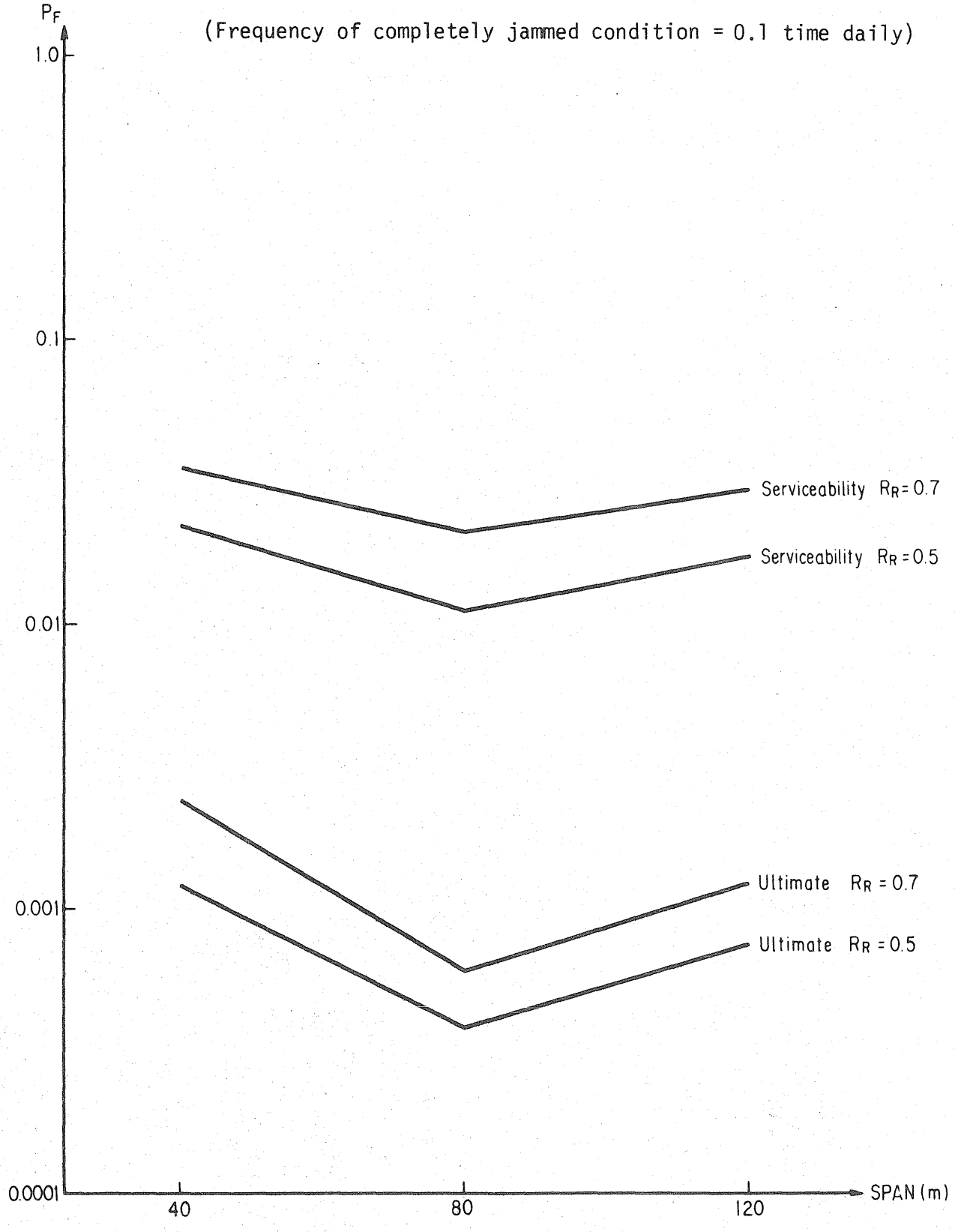

Fig. 4.3 PROBABILITY OF FAILURE OF BOX GIRDER BRIDGES (RELIABILITY-BASED DESIGN)

Using Eqs. (4.3) and (4.4), revised designs of box girders are obtained for spans of 40, 80, and 120m. The probabilities of failure of the girders are then calculated; the results are shonw in Fig. 4.3. From Fig. 4.3, it can be seen that designs obtained with Eqs. (4.3) and (4.4) will have more consistent reliability; that is, the probability for ultimate limit state is around 0.001 and the probability for unserviceability is around 0.01.

It should be emphasized that the results obtained above are, strictly speaking, applicable for major national highways in Japan, where traffic conditions are severe. For the design of bridges on local roads, lower load factors may be used, which may also be determined with the same approach used herein.

4.4 Reliability of Bridge Piers

In the design of bridge piers, earthquake is a dominant factor, especially in Japan. The major design stresses of bridge piers are the bending stresses due to earthquake; the axial compressive force due to dead load and live load is quite small. The determination of design seismic coefficient, therefore, is the most important problem in the aseismic design of bridge piers.

The determination of the design seismic coefficient should consider the large uncertainty and variability of maximum acceleration resulting from a strong motion earthquake. For example, according to Sect. 3.3, the distribution of the annual maximum acceleration due to earthquake in Tokyo is given as follows.

$$F_{II}(x) = \exp\left\{ - \left(\frac{15.3}{x}\right)^{1.53} \right\} \quad (\text{in cm/s}^2) \tag{4.5}$$

Applying Eq. (4.5), the maximum acceleration that can be expected in 50, 100, and 500 years are as follows:

50 years - Amax = 196 cm/s^2
100 years - Amax = 309 cm/s^2
500 years - Amax = 888 cm/s^2

These values may seem to be high; however, judging from the fact that high ground accelerations (recently, 1000 gals of acceleration was recorded in Japan) have repeatedly been recorded in Japan, they are not unreasonable.

From an economic point of view, it may not be possible to design bridge piers to resist such strong earthquake motions with high reliability. Currently, bridge piers are designed with a seismic coefficient of 0.2; according to the above results, this is equivalent to a return period of only 50 years.

The specification of the seismic coefficient does not, of itself, determines the safety of a bridge pier; it is the probability of failure of the resulting structure, designed with a given seismic coefficient, to the expected lifetime earthquake load that is important.

In this study, the probability that stresses due to the maximum seismic force during the lifetime of a bridge pier exceed the limit states stresses is examined, assuming that the pier response is elastic under strong motion and that dynamic limit state is equal to static limit state. The resulting probability is much higher than the actual probability of collapse or even of any damage. The reson is as follows.

1. Pier response will be reduced significantly under strong motion due to elasto-plastic behavior.
2. Dynamic limit state is much higher than static limit state.
3. Bridge systems are designed so that shoes of superstructures fail first under strong motion to prevent the failure of piers.

So, they represent only a measure of safety.

Usually, under the combination of extreme loads, the allowable stresses given in specifications are increased, recognizing the small chance of simultaneous occurrence of such combined loads. For example, the Specifications for Highway bridges in Japan permits the following allowable stresses in the design of steel bridge piers.

$D + L \leq 1400 kg/cm^2$

$D + L + EQ \leq 2100 kg/cm^2$

For the purpose of reliability analysis, bridge piers are designed assuming the same superstructures as those designed earlier in Sect. 4.2. The seismic coefficient used in the design is 0.2, which is currently used in the design of piers for downtown Tokyo. In this report, computer simulations were performed to determine the lifetime maximum combined load effects. In the computer simulation, D and L and the seismic coefficient are simulated independently, and subsequently the combined D, L and EQ load effects are calculated.

The information needed in the simulation and for the reliability analysis is as follows.

Dimensions of bridge piers -- Dimensions of the piers are determined by the computer program. Typical cross section and design conditions are those shown in Fig. 18.

Resistance -- As presented and discussed earlier in Sect. 4.3.

Loading -- The annual maximum earthquake acceleration is given by Eq. (4.5).

Information on dead load is as given earlier in Sect. 4.3. For live loads during an earthquake, the following three loading states are considered:

Loading state 1 : no vehicle on the bridge

Loading state 2 : running condition (normal traffic)

Loading state 3 : completely jammed condition

In the estimation of the lifetime maximum live load, only state 3 live load is significant; however, as the occurrence of loading state 3 is infrequent, the other live load loading states are important in the determination of the lifetime maximum combined loads.

The load intensity, that is the reaction force at the bridge support, of live load state 1 is zero.

The load intensity of state 2 live load was examined by K nihiro (1971), and the results are given by the lognormal distributions as follows.

Table 4.1 RATIO OF REAL REACTION FORCE IN STATE 2 TO DESIGN REACTION FORCE

Span	μ	σ	λ	ξ
40m	0.350	0.076	-1.073	0.215
80m	0.299	0.071	-1.235	0.234
120m	0.290	0.075	-1.270	0.254

The load intensity of state 3 live load can be obtained from results of the computer simulation described in Sect. 3.2. The results can be described with the lognormal distributions as follows.

Table 4.2 RATIO OF REAL REACTION FORCE IN STATE 3 TO DESIGN REACTION FORCE

Span	μ	σ	λ	ξ
40m	0.735	0.157	-0.330	0.211
80m	0.912	0.130	-0.102	0.142
120m	1.096	0.132	0.084	0.120

The composite distribution for the live loads in states 1, 2 and 3 may be given as follows.

$$FL(x) = P_1 \cdot FL_1(x) + P_2 \cdot FL_2(x) + P_3 \cdot FL_3(x) \quad (4.6)$$

where:

P_1, P_2, P_3 = the relative frequencies that the live loads are in state 1, 2 and 3

FL_1, FL_2, FL_3 = the lognormal distribution of the live loads in state 1, 2 and 3 respectively

P_1, P_2 and P_3 depend on the traffic condition at a site. Assuming that the loading state 3 occurs (on the average) 5 minutes daily, and $P_1=P_2$, then P_1, P_2 and P_3 can be given as follows.

$P_1=0.49826$ $P_2=0.49826$ $P_3=0.00384$

With the above information, the combined load effect of D, L and EQ can be simulated annually, from which lifetime maximum combined loads over a life of 50 years can be obtained. The probabilities that stresses due to the maximum combined load effects exceed the limit states stresses (as defined earlier) are summarized in Fig. 4.4.

From Fig. 4.4, the following observations may be made.

First, the probabilities that stresses due to the maximum combined load effects exceed the limit states stresses are pretty high. However, as discussed earlier, the probability of collapse or of damage is much smaller.

Secondly, the probabilities do not depend significantly on the height of piers; however, they depend on the spans of superstructures, because the load ratios depend significantly on the spans.

4.5 Reliability-Based Design Requirements for Bridge Piers

The total design load intensity of bridge piers is composed of the followings:

Axial force due to dead weight and live load.

Bending moment due to

dead weight x moment length x seismic coefficient and

live load x moment length x seismic coefficient.

Therefore, even though it is difficult to determine the actual load ratios, it is reasonable to assume that the safety of bridge piers can be expressed approximately as a function of the load ratio of the axial live load to the axial dead

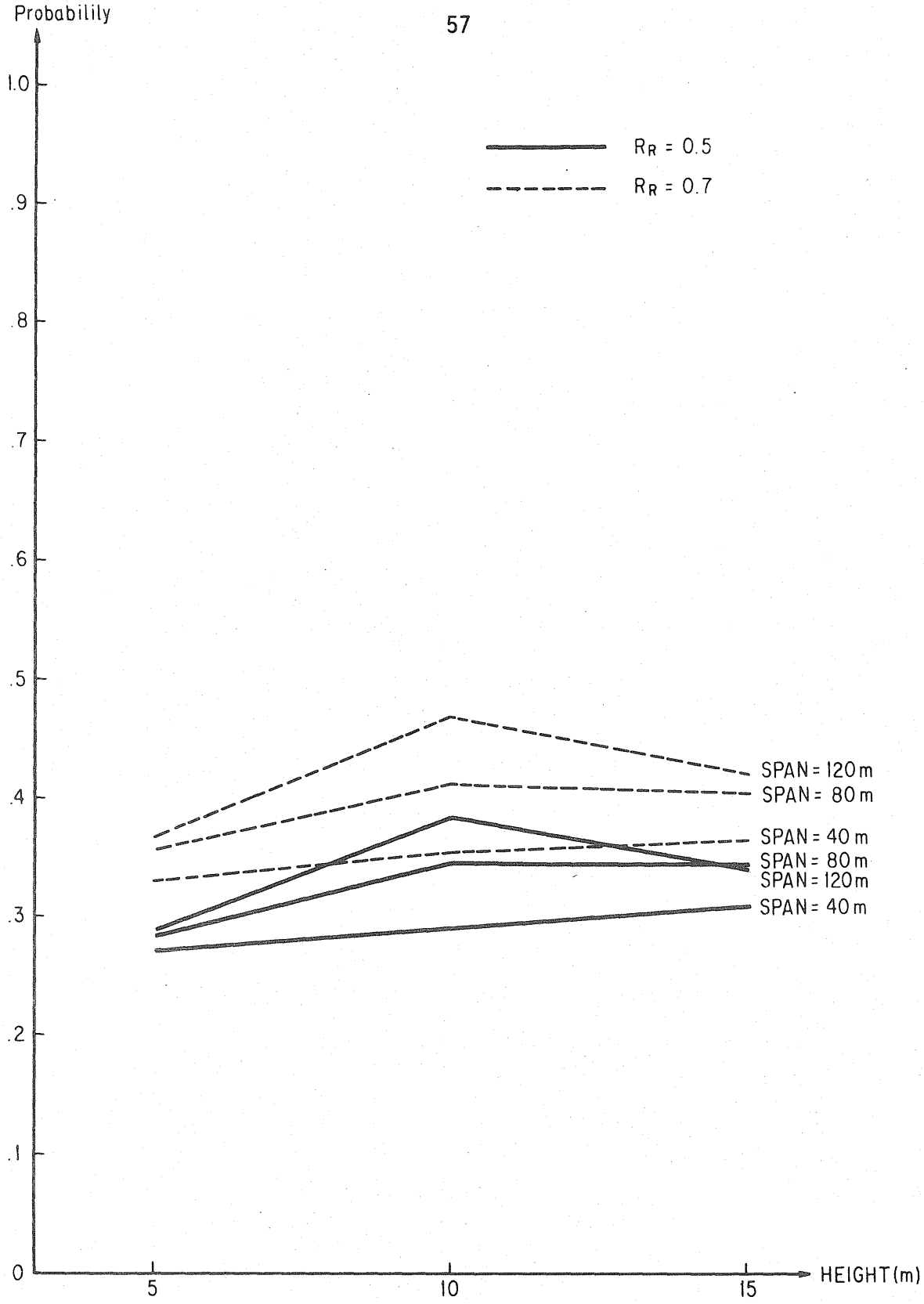

Fig. 4.4 MEASURE OF SAFETY FOR BRIDGE PIERS **

** The probability that stresses due to lifetime maximum combined load effects exceed the ultimate limit state stresses.
The probability of collapse or of damage is much smaller.

load, because the arm length and the seismic coefficient for both loads are nearly the same.

For example, for piers with 10m height, safety factors that will ensure the probability (defined in Sect. 4.4) of 0.3 for bridge piers with R_R=0.5 are as follows.

Spans	Axial load ratios (L/D)	Safety factors corresponding to probability=0.3
40m	0.733	1.067
80m	0.392	1.237
120m	0.208	1.288

From the above relations, the following safety factors may be used to give consistent safety to bridge piers:

$$\text{Safety Factor} = 1.388 - 0.431\ (L/D) \tag{4.7}$$

where L and D are axial design loads.

To ascertain the consistency of Eq. (4.7), the computer simulations were performed for the bridge piers designed according to Eq. (4.7). The design nominal resistances are the same as those defined in Sect. 4.2, that is;

for $R_R = 0.5$ $\quad R^* = 0.982 \cdot \sigma y$

for $R_R = 0.7$ $\quad R^* = 0.854 \cdot \sigma y$

The calculated probabilities for the piers designed in accordance with Eq. (4.7) are shown in Fig. 4.5. From these results, it can be seen that Eq. (4.7) gives nearly consistent safety to bridge piers for every combinations of spans, heights and breadth-to-thickness ratios. Although the safety level of the bridge piers designed according to Eq.(4.7) is not known (as explained in Sect. 4.4), it is the same as the safety level of the pier with 40m of span and 5m of height designed according to the present code.

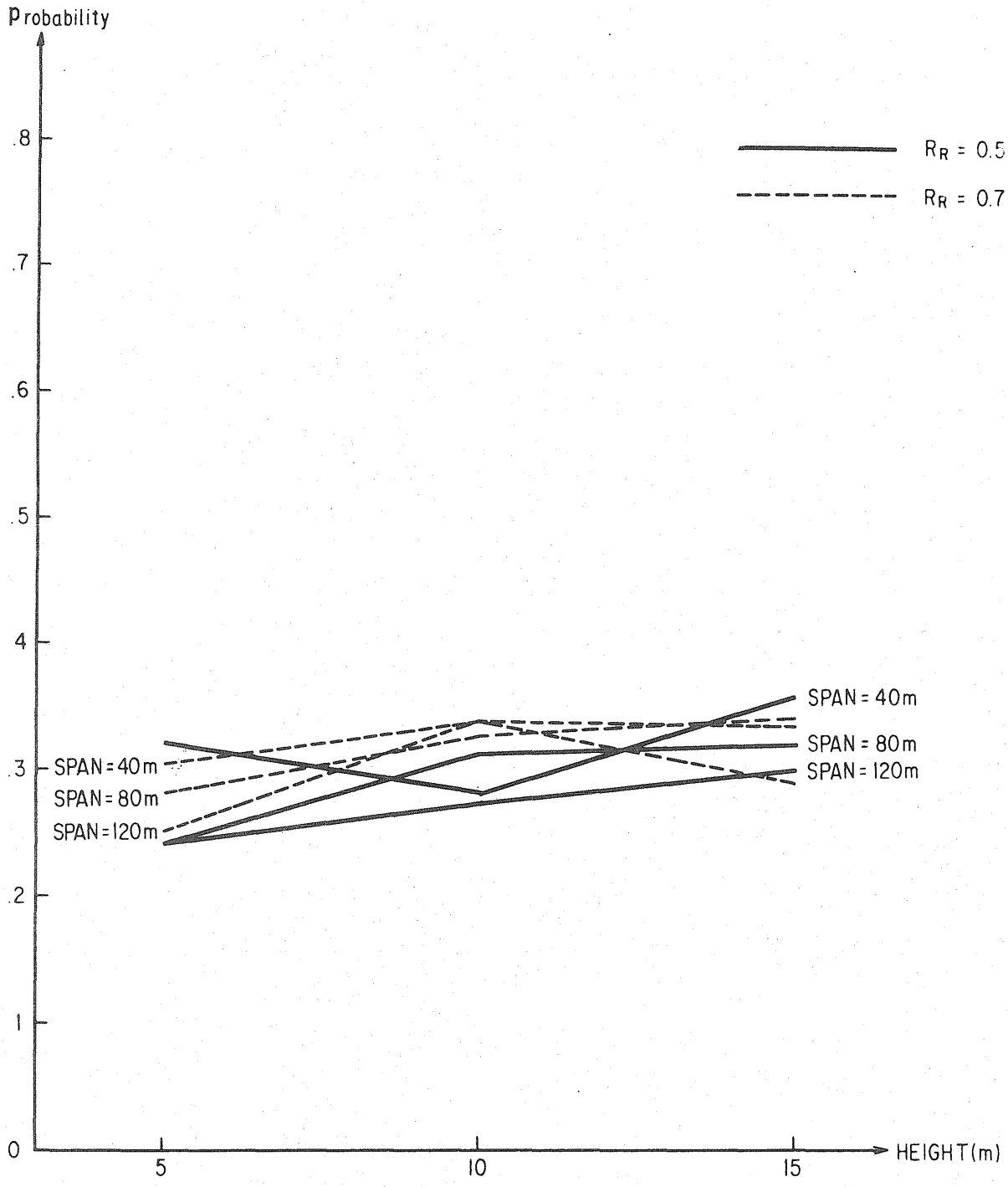

Fig. 4.5 MEASURE OF SAFETY FOR BRIDGE PIERS **
(RELIABILITY-BASED DESIGN)

** The probability that stresses due to lifetime maximum combined load effects exceed the ultimate limit state stresses.
The probability of collapse or of damage is much smaller.

CHAPTER 5

CONCLUSIONS

The levels of safety of box girders and bridge piers designed according to the present code in Japan appear to vary widely. This is largely due to the large uncertainties in the live load and in the earthquake load, which require reliability analysis.

In the design of box girders, the following design formulas may be adopted to achieve acceptable failure probabilities of 0.001 against ultimate limit and 0.01 for unserviceability.

$$\begin{aligned} &\text{For ultimate limit} && 0.95\ R \geq 1.15\ D + 2.30\ L \\ &\text{For serviceability} && 0.95\ R \geq 1.10\ D + 2.20\ L \end{aligned} \tag{5.1}$$

where:

$R = -0.920R_R + 0.277R_R^2 - 0.046R_R^3 + 1.378$; for ultimate limit

$R = -1.578R_R + 1.022R_R^2 - 0.267R_R^3 + 1.294$; for serviceability

In the design of bridge piers, the following design formula may be used to insure the same safety level as that of the pier with 40m of span and 5m of height and R_R=0.5 designed according to the present code.

$$R \geq (1.388 - 0.431 \cdot (L/D)) \cdot (D + L + EQ) \tag{5.2}$$

where:

$$R = -0.920R_R + 0.277R_R^2 - 0.046R_R^3 + 1.378$$

Equations (5.1) and (5.2) are derived to give the same reliability to structures as those implied in designs obtained with the present code, at a certain combination of span, height and other design variables. Before the formulas are applied to actual structural design, the acceptable levels of safety should be discussed from an economic point of view. If other levels of safety are deemed necessary, the appropriate load and resistance factors in the design equations may be altered systematically using the approach proposed herein.

LIST OF REFERENCES

1. AASHTO, "Specifications for Highway Bridges" 1977.

2. Ang, A.H.-S., "Structural Reliability and Probability Based Design", Japan Society for the Promotion of Science, April 1976.

3. Ang, A.H.-S. and Tang, W., "Probability Concepts in Engineering Planning and Design", John Wiley & Sons, 1975.

4. Ang, A.H.-S. and Cornell, C.A., "Reliability Basis of Structural Safety and Design", Journal of the Structural Division, ASCE, NO. ST9, 1974.

5. ASCE-AASHO Task Committee on Flexural Members, "Progress Report on Steel Box Girder Bridges", Journal of the Structural Division, ASCE, NO. ST4, 1971.

6. Cornell, C.A., "Structural Safety Specifications based on Second-Moment Reliability Analysis", Final Report, IABSE, 1969.

7. Hattori, S., "Earthquake Danger in the Whole Vicinity of Japan", Report of the Building Research Institure, No. 81, June 1977.

8. Japan Road Association, "Specifications for Highway Bridges" 1973.

9. Japan Road Association, "Specifications for Aseismic Design of Highway Bridges" 1972.

10. Kanai, M., "Experimantal Research on the Ultimate Strength of Stiffened Plates", Yearly Report of the P.W.R.I., 1978.

11. Kanai, M., "Reliability Analysis of Steel Bridges", Report of the P.W.R.I. No. 1225, 1977.

12. Kanai, M., "Research on Load Factor Design Method of Highway Bridges" Yearly Report of the P.W.R.I., 1978.

13. Kunihiro, T., "Research on Design Live Load", Report of the P.W.R.I. No. 701, 1971.

14. Larry, A., "Steel Box Girder Bridges", Engineering Journal, American Institute of Steel Construction, Fourth Quarter, 1973.

15. Lind, N.C., "Structural Reliability and Codified Design", SM Study No.3., Solid Mech. Div., Univ. of Waterloo, 1970.

16. Merrison Committee, "Inquiry into the Basis of Design and Method of Erection of Steel Box Girder Bridges", 1973.

17. P.W.R.I., "Research on Design Live Load on Highway Bridges", Report of the P.W.R.I. No. 936, 1973.

18. P.W.R.I., "Report on Aseismic Design Method", Report of the P.W.R.I. No. 1135, 1977.

19. Task Committee on Orthotropic Plate Bridges of the Committee on Metals of the Structural Division, "Commentary on Orthotropic-Deck Bridge Specification" Journal of the Structural Division, ASCE, No. ST1, 1974.

20. Wen, Y.-K., "Probability of Extreme Load Combination", 4th International Conference on Structural Mechanics in Reactor Technology", August 1977.

21. Wen, Y.-K., "Statistical Combination of Extreme Loads", Journal of the Structural Division, ASCE, No. ST5, 1977.